

Article

## The life and times of *Pteridinium simplex*

Simon A. F. Darroch\* , Brandt M. Gibson, Maggie Syversen, Imran A. Rahman, Rachel A. Racicot, Frances S. Dunn, Susana Gutarra, Eberhard Schindler, Achim Wehrmann, and Marc Laflamme

**Abstract.**—*Pteridinium simplex* is an iconic erniettomorph taxon best known from late Ediacaran successions in South Australia, Russia, and Namibia. Despite nearly 100 years of study, there remain fundamental questions surrounding the paleobiology and paleoecology of this organism, including its life position relative to the sediment–water interface, and how it fed and functioned within benthic communities. Here, we combine a redescription of specimens housed at the Senckenberg Forschungsinstitut und Naturmuseum Frankfurt with field observations of fossiliferous surfaces, to constrain the life habit of *Pteridinium* and gain insights into the character of benthic ecosystems shortly before the beginning of the Cambrian. We present paleontological and sedimentological evidence suggesting that *Pteridinium* was semi-infaunal and lived gregariously in aggregated communities, preferentially adopting an orientation with the long axis perpendicular to the prevailing current direction. Using computational fluid dynamics simulations, we demonstrate that this life habit could plausibly have led to suspended food particles settling within the organism's central cavity. This supports interpretation of *Pteridinium* as a macroscopic suspension feeder that functioned similarly to the coeval erniettomorph *Ernietta*, emblematic of a broader paleoecological shift toward benthic suspension-feeding strategies over the course of the latest Ediacaran. Finally, we discuss how this new reconstruction of *Pteridinium* provides information concerning its potential relationships with extant animal groups and state a case for reconstructing *Pteridinium* as a colonial metazoan.

Simon A. F. Darroch\*, Brandt M. Gibson†, and Maggie Syversen. Department of Earth & Environmental Sciences, Vanderbilt University, Nashville, Tennessee, U.S.A. E-mail: [simon.a.darroch@vanderbilt.edu](mailto:simon.a.darroch@vanderbilt.edu), [brandt.m.gibson@vanderbilt.edu](mailto:brandt.m.gibson@vanderbilt.edu), [maggussyversen@LIVE.COM](mailto:maggussyversen@LIVE.COM). \*Present address: Senckenberg Research Institute and Museum of Natural History, Frankfurt, Germany. †Present address: Department of Chemical and Physical Sciences, University of Toronto Mississauga, Mississauga, Ontario, Canada.

Imran A. Rahman and Susana Gutarra. Natural History Museum, London, London, U.K. E-mail: [imran.rahman@nhm.ac.uk](mailto:imran.rahman@nhm.ac.uk), [susana.gutarra-diaz@nhm.ac.uk](mailto:susana.gutarra-diaz@nhm.ac.uk)

Rachel A. Racicot‡. Department of Biology, Vanderbilt University, Nashville, Tennessee, U.S.A. E-mail: [rachel.a.racicot@vanderbilt.edu](mailto:rachel.a.racicot@vanderbilt.edu).

Frances S. Dunn. Oxford University Museum of Natural History, Oxford, U.K. E-mail: [frances.dunn@oum.ox.ac.uk](mailto:frances.dunn@oum.ox.ac.uk)  
Eberhard Schindler. Senckenberg Research Institute and Museum of Natural History, Frankfurt, Germany.  
E-mail: [eberhard.schindler@senckenberg.de](mailto:eberhard.schindler@senckenberg.de)

Achim Wehrmann. Senckenberg am Meer, Marine Research Department, Wilhelmshaven, Germany. E-mail: [achim.wehrmann@senckenberg.de](mailto:achim.wehrmann@senckenberg.de)

Marc Laflamme. Department of Chemical and Physical Sciences, University of Toronto Mississauga, Mississauga, Ontario, Canada. E-mail: [marc.laflamme@utoronto.ca](mailto:marc.laflamme@utoronto.ca)

Accepted: 12 January 2022

\*Corresponding author.

### Introduction

The latest Neoproterozoic (~571–539 Ma) Ediacara biota is an enigmatic collection of organisms that represents the first major radiation of complex, macroscopic eukaryotes, which disappeared before the Cambrian (Xiao

and Laflamme 2009; Laflamme et al. 2013; Darroch et al. 2015, 2018a,b; Droser and Gehling 2015; Liu et al. 2015; Muscente et al. 2019). Reconstructing the paleobiology, paleoecology, and biological affinities of the Ediacara biota is thus key to understanding the origins of the modern marine biosphere

© The Author(s), 2022. Published by Cambridge University Press on behalf of The Paleontological Society. This is an Open Access article, distributed under the terms of the Creative Commons Attribution licence (<https://creativecommons.org/licenses/by/4.0/>), which permits unrestricted re-use, distribution, and reproduction in any medium, provided the original work is properly cited.

0094-8373/22

(Darroch et al. 2018b). Despite an emerging consensus arguing for animal affinities for at least some members of the Ediacara biota, their unusual and non-analogue body plans mean a majority of these taxa still occupy uncertain positions on the eukaryotic tree of life, hindering efforts to decipher their biology and obscuring our understanding of the evolutionary and ecological dynamics leading up to the Cambrian explosion of animals (Darroch et al. 2018b; Dunn et al. 2018). This uncertainty has rendered phylogenetic approaches to understanding life habit and ecology uninformative. However, in recent years, a suite of new modeling-based approaches have allowed us to elucidate the function of several Ediacaran organisms (Mitchell et al. 2015; Rahman et al. 2015; Darroch et al. 2017; Mitchell and Kenchington 2018; Gibson et al. 2019; Muscente et al. 2019), in turn providing information about the character of Neoproterozoic food webs, patterns of energy transfer, and the timing of key geobiological step changes (Rahman et al. 2015; Gibson et al. 2019, 2021b; Cracknell et al. 2021). In this study, we reexamine the paleobiology and paleoecology of the Ediacaran erniettomorph taxon *Pteridinium simplex* (Gürich 1930b) using a combination of field paleoecological and sedimentological observations, fossil material, and computational fluid dynamics (CFD). While a majority of Ediacara biota apparently became extinct at the boundary between the White Sea and Nama assemblages ~548 Ma, *Pteridinium* is one of the few taxa that persisted until the end of the Ediacaran and thus has the potential to shed valuable new light on ecological dynamics during a key part of the Ediacaran-Cambrian transition (Darroch et al. 2018b).

*Erniettomorpha*.—The Erniettomorpha are united by a shared mode of construction based on repeated tubular “modules” that are smooth, typically unbranched, and cylindrical in shape (Erwin et al. 2011) (Fig. 1). Modules typically alternate from side to side along the central midline (i.e., “glide symmetry”), which demonstrates that these organisms are not truly bilaterally symmetrical (Erwin et al. 2011). Recent work has considered the Erniettomorpha to be a clade, sister to the Rangeomorpha (Pflug 1972a; Dececchi et al. 2017);

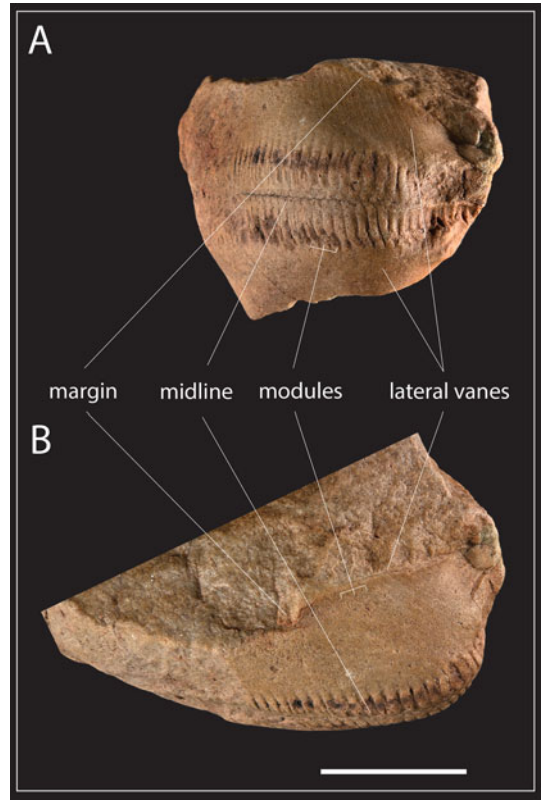


FIGURE 1. Neotype specimen (SMF XXX 660f) of *Pteridinium simplex* housed in the Senckenberg Forschungsinstitut und Naturmuseum in Frankfurt, Germany, shown in: A, dorsal view; and B, from the side in inferred life position (see, e.g., Meyer et al. 2014a). Specimen illustrates key features of *Pteridinium*, including construction from tubular modules, arranged into two lateral vanes that join at a central midline (or “seam”). Modules are offset either side of the midline (“glide symmetry”). At each end of the organism, the lateral vanes join to form a keeled “canoe” shape, which is commonly seen bisected by a third, upright vane (not preserved in this specimen). Scale bar, 5 cm.

however, this is not universally agreed upon (Hoyal-Cuthill and Han 2018). Pflug (1970a,b) erected the phylum Petalonamae to encompass all frondose Ediacarans such as *Charnia*, *Rangea*, *Arborea*, and *Pteridinium* (an opinion shared by Glaessner 1979), but this assignment remains uncertain due to disagreements over whether the similarities between these fronds are the result of shared ancestry (e.g., Hoyal-Cuthill and Han 2018) or convergence (e.g., Laflamme and Narbonne 2008a,b). “Petalonamae” has subsequently been used in other ways, for example, to describe a subsection of these fronds (e.g.,

Grazhdankin 2014) or to refer to a group also encompassing non-frondose forms like *Dickinsonia* (Hoyal-Cuthill and Han 2018), making it the senior synonym to “Vendobionta” and rendering “Petalonamae,” as originally conceived, paraphyletic. Together, these differing hypotheses have introduced ambiguity over the meaning of the term “Petalonamae.” Here, we follow Decechi et al. (2017) in considering the Erniettomorpha—including *Ernietta*, *Swartpuntia*, and *Pteridinium*—to be monophyletic.

Erniettomorph taxa display a number of body architectures and are inferred to have occupied a wide variety of life modes, including recumbent epifaunal “carpet”-like forms (e.g., *Phyllozoon hanseni*; see Jenkins and Gehling 1978; Gehling and Runnegar 2021), partially infaunal bag-shaped forms (e.g., *Ernietta plateauensis*; Elliott et al. 2016; Ivantsov et al. 2016), and upright frondose forms attached to the substrate via a holdfast (e.g., *Swartpuntia germsi*; Narbonne et al. 1997). Current evidence thus suggests that Erniettomorpha comprise an ecologically diverse collection of organisms that flourished for ~20 Myr in the latest Neoproterozoic and possessed no characters (at least, that are universally accepted) that would place them within Metazoa. Crucially, the Erniettomorpha (including *Pteridinium*) are one of only three Ediacaran clades that persisted at least until the base of the Cambrian, with many other iconic Ediacaran groups disappearing in a putative first pulse of Ediacaran extinction at the boundary between the White Sea and Nama assemblages ~548 Ma (Schiffbauer et al. 2016; Darroch et al. 2018b; Muscente et al. 2019). Darroch et al. (2018b) suggested that this may have been due to the Erniettomorpha being ecological generalists (and thus more able to survive or avoid ecological stressors associated with extinction); however, this hypothesis is currently untested. Determining the paleobiology and paleoecology of erniettomorph taxa therefore has the potential to shed light not only on ecological dynamics in the very latest Ediacaran (which is now recognized as having much in common with the earliest Cambrian, and thus part of the greater Cambrian radiation; see Darroch et al. 2016, 2018b; Wood et al. 2019), but also on the

drivers of latest Ediacaran turnover events (Darroch et al. 2018b; Gibson et al. 2021b).

*Pteridinium* itself has been assigned to a variety of metazoan groups. Richter (1955) suggested that it may represent an early example of the Gorgonacea; however, this was likely a response to considering the frondose taxa *Rangea* and *Arborea* both octocorals and close relatives. Glaessner and Wade (1966) put forward an assignment to the Octocorallia (Anthozoa), but were reluctant to support the Pteridiniidae (Family) assignment, given the fragmentary nature of the material. Gehling (1991) suggested that, due to the major morphological differences between *Pteridinium* and other fronds, it was unlikely to be closely related to them, and instead proposed they could represent macrophytic algae or even members of the Vendozoa (later Vendobionta; Seilacher 1992; Buss and Seilacher 1994), an idea that was supported by Grazhdankin and Seilacher (2002). Fedonkin (1990), Ivantsov and Fedonkin (2002), and Fedonkin and Ivantsov (2007) argued that the three-vented architecture of *Pteridinium* meant it was best considered as a member of the “Trilobozoa” (together with other threefold Ediacaran taxa such as *Tribrachidium* and *Anfesta*). However, given the morphological and taphonomic evidence, we follow Erwin et al. (2011) in considering *Pteridinium* as an erniettomorph.

*Pteridinium simplex*.—*Pteridinium simplex* (Gürich 1930b) is an erniettomorph best known from the Nama-aged sediments in southern Namibia (Gürich 1929, 1930a,b, 1933; Richter 1955; Pflug 1970a,b, 1972a,b, 1973; Elliott et al. 2011; Meyer et al. 2014a), as well as the White Sea-aged sediments in South Australia (Glaessner and Wade 1966) and Russia (Fedonkin 1981). *Pteridinium simplex* is trifoliate, with three vanes joined at a central seam. In the most recent reconstructions based on material from Namibia (Kliphoek Member, Dabis Formation), two vanes are arranged laterally, but curved and joined at each end to form an elongate canoe shape, with an upright third vane that splits the central cavity in half (see, e.g., Pflug 1973; Grazhdankin and Seilacher 2002; Meyer et al. 2014a). This third vane has typically been reconstructed as having originally been flush with the edges of the central cavity (see, e.g.,

Meyer et al. 2014a); however, it is also plausible that this upright vane could have been extended higher into the water column, similar to what has been reconstructed for the lateral margins of *Ernietta* (see, e.g., Ivantsov et al. 2016; Gibson et al. 2019).

Although there has been considerable disagreement surrounding the life position of *Pteridinium* (see, e.g., Jenkins 1985; Crimes and Fedonkin 1996; Grazhdankin and Seilacher 2002; Runnegar 2021), the most common reconstructions interpret the organism as recumbent, lying either at or partially buried beneath the sediment–water interface, similar to *Ernietta* (Ivantsov et al. 2016; Gibson et al. 2019). Suggestions made by Grazhdankin and Seilacher (2002) that *Pteridinium* may have been entirely infaunal and growing while buried within the sediment were largely refuted by Elliott et al. (2011), who noted no evidence of sediment displacement around fossils—an expectation for an organism growing by sediment pervasion. There is likewise no evidence that *Pteridinium* fossils represent the principal or propagative part of an originally upright organism nor is there any evidence that it is a dissociated element of a triradialomorph taxon such as *Tribrachidium* (sensu Runnegar 2021).

Reexamination of the fossil material housed in the Senckenberg Forschungsinstitut und Naturmuseum Frankfurt, along with observations of fossil surfaces made in the field, allow us to test key tenets of this model and help establish the life habit of *Pteridinium simplex*, along with the paleoenvironments in which it is typically found. This evidence-based reconstruction in turn informs our choice of modeling parameters in CFD experiments (including inlet velocities, model orientations, etc.), allowing us to elucidate its behavior in moving fluids and shed light on its paleobiology.

### Museum Specimens

The fossil specimens examined here are housed in the Senckenberg Forschungsinstitut und Naturmuseum Frankfurt, Germany. The material was collected by Richard Kräusel (Senckenberg, Frankfurt) in 1954 from sediments belonging to the Kliphoek Member (Dabis Formation) on Farms Plateau, Aar,

Kuibis, and Kalkfontein in the Witputs Subbasin in southern Namibia (localities illustrated in Supplementary Fig. 1). This is broadly equivalent to the fossil material studied by Pflug (1970a,b, 1972b, 1973), Grazhdankin and Seilacher (2002), Elliott et al. (2011), and Meyer et al. (2014a,b). The slabs (loose blocks that were likely derived from the outcropping rocks underneath) were handed to Rudolf Richter, who subsequently published a detailed description (Richter 1955). The collection comprises about 35 individual specimens and slabs that include well-preserved *Pteridinium simplex*, *Ernietta plateauensis*, and *Rangea schneiderhoehni*, as well as a possible small and fragmentary *Ausia*. Richter (1955) selected one of these specimens as a neotype for *Pteridinium* (see Fig. 1), as a substitute for the holotype that was destroyed in World War II. In addition to reexamining and refiguring this material, we produced polished cross sections and thin sections to describe the sedimentological context of key fossil specimens.

**Geology.**—The Dabis Formation in the Witputs Subbasin is subdivided into the Kanies, Mara, Kliphoek, and Aar Members. Kliphoek Member sandstones are thought to have been deposited with regional sea-level fall/lowstand, which caused siliciclastic shorelines to prograde over carbonates belonging to the underlying Mara Member (Saylor et al. 1995). Sandstones in these units are typically medium grained and cross-bedded and likely represent upper-shoreface delta- and tide-influenced paleoenvironments (Saylor et al. 1995; Grotzinger and Miller 2008; Hall et al. 2013; Maloney et al. 2020). Fossils are relatively common in the Aar Member in the vicinity of the Aar Plateau (see Hall et al. 2013), which is composed of interbedded sandstones and shales with minor limestones. *Pteridinium* fossils, however, are most common at the top of the Kliphoek Member and within the “Aarhauser Sandstone” unit ~10 m above the base of the Aar Member and characterized by gutter casts, storm beds, and tabular sandstone horizons thought to represent sheet-flood events (Elliott et al. 2011; Hall et al. 2013; Vickers-Rich et al. 2013; Meyer et al. 2014a).

**Biostratinomy and Sedimentological Context.**—Slabs preserve *Pteridinium* fossils in a range of



FIGURE 2. SMF 20674; slab preserving a dense accumulation of *Pteridinium simplex* in three dimensions. A, View of slab base with more than 10 individuals of varying sizes present; note highly variable long-axis orientations among individuals, as well as the large size variation, and attitude within the sediment. The vast majority of seams are preserved as negative relief furrows. B, C, View of slab in cross section in two views and in inferred original orientation toward the top of the slab. Individual *P. simplex* preserved predominantly in massive sediment toward the base of the slab, which is capped by a thin (2–3 cm) horizon of laminated quartzitic sandstone (l.) with underlying scour structures (sc.). D, Close-up of two individuals visible in A, illustrating differences in orientation and attitude within the bed. E, Close-up of an individual visible in C, showing well-preserved glide symmetry linking the two lateral vanes, created by regular lateral offset in segments either side of the seam. Scale bars, 2 cm.

styles, suggesting a spectrum of biostratinomic contexts. At one end of the spectrum are specimens preserved in three dimensions, where individuals are folded, deformed, and with central (i.e., upright) vanes frequently exposed (Figs. 2, 3). These slabs also typically exhibit a range of sedimentary structures, including small-scale cross-bedding, even lamination, tabular cross stratification, slumping, and scours (Fig. 2). Both the style of fossil preservation and the sedimentology thus support the interpretation that these fossils were buried and preserved as part of wave-/storm-induced density- or mass flow deposits in a shallow-

marine setting (Hall et al. 2013; Meyer et al. 2014a,b).

At the other end of the spectrum are specimens preserved in two dimensions on bed tops (“negative epirelief”; Fig. 4); in these individuals, the central axis and two horizontal vanes are typically visible (missing only the outermost edges), with little to no evidence for a third, upright vane. These slabs also preserve a different suite of sedimentological structures, most notably millimeter-scale laminations indicating a comparatively low-energy depositional environment. Occupying an approximate intermediate state between these



FIGURE 3. SMF XXX 660k; slab preserving an accumulation of *Pteridinium simplex* in three dimensions. A, View of slab base with approximately five individuals of varying sizes present; as with Fig. 2, note variable long-axis orientations and size variation among fossils and seams preserved as negative relief furrows. Loose fragment in top left (fr) comes away to reveal the third (i.e., central) vane. B, Close-up of an individual visible in A possessing several partially deformed, interleaved, or twisted segments (i). C, Slab seen from oblique angle, showing the split (br) formed along medial vane and preserving fossil impressions on both sides of the break. D, Close-up of loose fragment, with both lateral (h) and central (v) vanes labeled. Inset E, detail of the seam where lateral and medial vanes join, illustrating offset of segments and pronounced kink in segments close to the seam. F, Counterpart to face shown in D, again illustrating the seam between lateral and medial vanes and pronounced kink in segments located centrally. Scale bars, 2 cm.

two end-members are slabs that preserve multiple individuals in three dimensions (frequently preserving a third, upright vane) but appear less folded and deformed, with a greater degree of long-axis alignment.

A thin section cut from SMF XXX 660i (Figs. 5, 6) reveals that the two individual

*Pteridinium* in this slab are preserved in mature fine-grained sandstone composed of overwhelmingly subangular to subrounded quartz grains, typically 50–150  $\mu\text{m}$  in diameter and with a mean grain size of 110  $\mu\text{m}$ . Mica is common within the matrix, displaying a mixture of long-axis orientations that range from bed-



FIGURE 4. SMF XXX 660q; A, slab preserving two large individual *Pteridinium simplex* as two-dimensional negative epirielief impressions on the slab top surface. Note (in the larger individual in particular) clear preservation of segments closer to the seam, indistinct margins of the lateral vanes, and non-preservation of the raised central vane. B, Close-up view of area highlighted in A, illustrating clear offset of segments across the seam separating lateral vanes, and split/deformed segments (i) resembling the counterpart to those shown in Fig. 2B. C, Slab seen in cross section, showing thin, continuous laminae present across the width of the slab. Scale bar in A, 2 cm.

parallel to random, suggesting a mixture of mica grains deposited contemporaneously within the sediment, as well as some that grew later with diagenesis and metamorphism.

Opaque components and lithic fragments also occur rarely. The thin section reveals the presence of a fining-up sequence capped with a thin, slightly inclined clay layer,

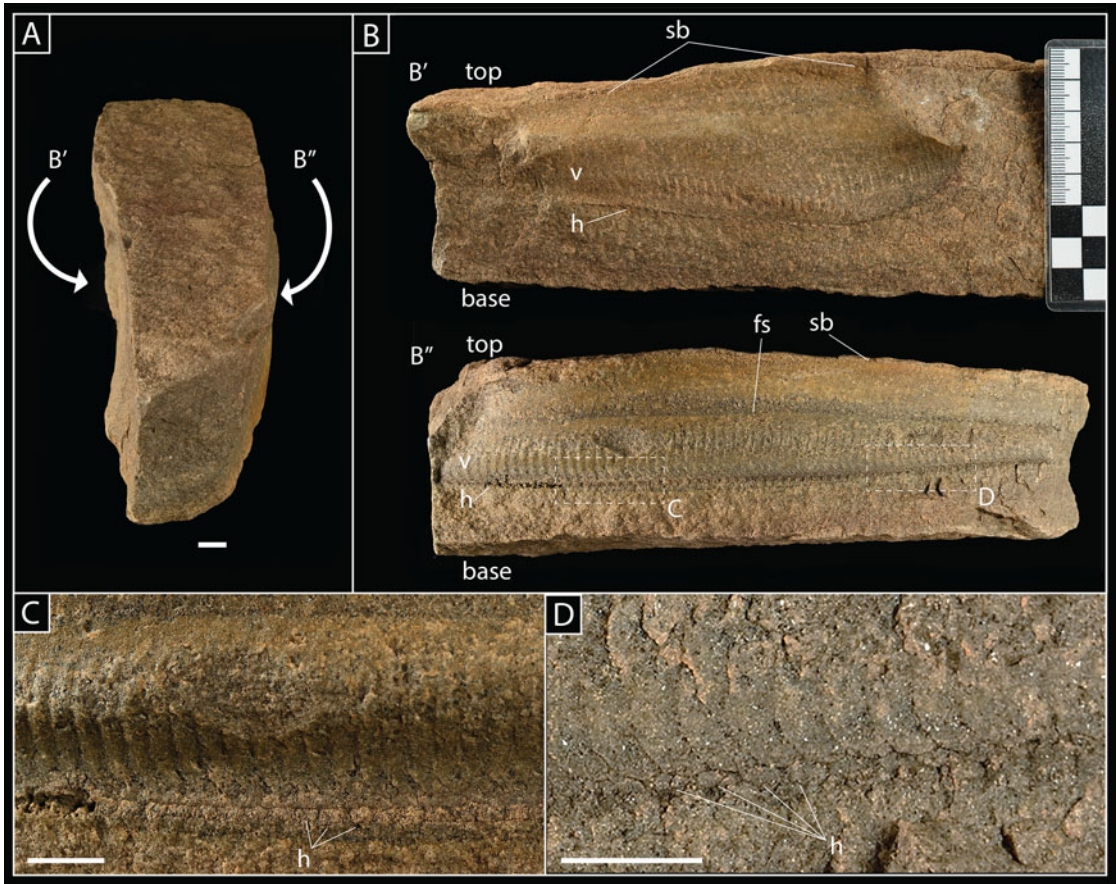


FIGURE 5. SMF XXX 660i; single slab preserving two individual *Pteridinium simplex* in three dimensions and in inferred life position with long axes parallel on either side of slab. A, Slab viewed from top, with the position of *P. simplex* fossils (B' and B'') indicated. B, Lateral views of *P. simplex* on either side of slab, exposing central vanes (v) and traces of individual modules, as well as the junction with lateral vanes (h), which are oriented approximately parallel to bedding where they meet the central vane. Also indicated is the presence of a prominent sedimentary boundary (sb) and fining-up sequence (fs); note that, in both specimens (B' and B''), modules extend through this latter boundary, indicating that the central vane was likely raised above the sediment–water interface in life. C, D, close-up views of the junction between lateral and horizontal vanes; outline of horizontal vanes coming out of the plane of view (h) clearly visible. Scale bars, 1 cm.

suggesting a sedimentary hiatus and the presence of at least two depositional events within the slab.

### Field Observations

Additional clues to establishing the original life habit of *Pteridinium simplex* come from contrasting the morphology and biostratinomy of specimens housed in the Senckenberg collections with those from well-documented field localities. Specifically, we focus on fossil *Pteridinium* from Farm Swartpunt, preserved in terminal Ediacaran

sediments belonging to the Nama Group of southern Namibia.

**Geology.**—Ediacaran fossils from Farm Swartpunt are preserved in sediments belonging to the Spitskop Member of the Urusis Formation within the Witputs Subbasin (Grotzinger et al. 1995; Narbonne et al. 1997; locality and stratigraphic summary shown in Supplementary Fig. 1). Ash beds bracketing fossil horizons originally dated by Grotzinger et al. (1995) were redated by Linnemann et al. (2019), yielding updated ages between  $540.095 \pm 0.099$  Ma and  $538.99 \pm 0.21$  Ma. Horizons preserving soft-bodied Ediacara biota also

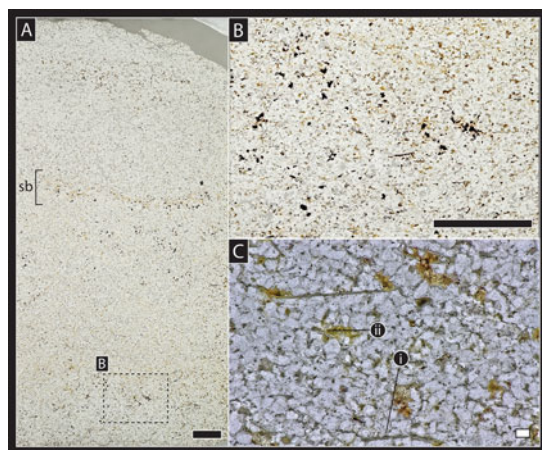


FIGURE 6. Sedimentology of slab SMF XXX 660i illustrated in thin section. A, Entire thin section in vertical profile, highlighting a clay-rich layer (sb) marking the top of a fining-upward sequence (corresponding to the sedimentary boundary shown in Fig. 4A). B, Enlarged area (shown in A) illustrating overall horizontal fabric created by bed-parallel alignment of elongate mica grains. C, High-resolution image illustrating subangular to subrounded grain boundaries, as well as micas that appear to both lie between sand grains (i) and overgrow sand grains (ii), suggesting a mixture of depositional and metamorphic/diagenetic origins. Black scale bars, 5 mm; white scale bar, 100  $\mu\text{m}$ .

occur beneath the last appearance datum of *Cloudina* and *Namacalathus* in the basin as well as the first appearance datum of *Treptichnus pedum* in the overlying Nomtsas Formation, establishing these horizons as latest Ediacaran (Narbonne et al. 1997; Darroch et al. 2015, 2020; although also see Linnemann et al. [2019] for a slightly different ichnostratigraphy).

The Spitskop Member comprises a mixed carbonate–siliciclastic succession that principally records inner-ramp highstand ribbon limestones and mid- to outer-ramp transgressive siliciclastics (Grotzinger and Miller 2008; Wood et al. 2015), deposited under persistently oxygenated conditions (Darroch et al. 2015; Wood et al. 2015). The fossils themselves are preserved in siliciclastic horizons toward the top of the cuesta, exposed as three prominent ridges that are interspersed with scree material (Narbonne et al. 1997; Darroch et al. 2015). Soft-bodied Ediacara biota are preserved in place in a number of horizons in rippled medium- to coarse-grained sandstone (including on the

top of the first two ridges, equivalent to fossil beds A and B of Narbonne et al. [1997]), as well as within thin-bedded green siltstones and yellow-green medium-grained sandstone horizons with minor carbonate interbeds (Darroch et al. 2015). Both Narbonne et al. (1997) and Darroch et al. (2015) reported a change in bedding from horizontal to subvertical at the contact between fossil-bearing siliciclastic horizons and underlying carbonate, interpreted by Narbonne et al. (1997) as a “mega slump.” These apparently slumped horizons do, however, contain an intact stratigraphy composed of mudstones, siltstones and sandstones with abundant ripple cross-lamination, hummocky cross-bedding, and gutter casts (Narbonne et al. 1997; Darroch et al. 2015), and they have been interpreted as recording the progradation of a wave- and storm-influenced delta (Narbonne et al. 1997).

*Biostratigraphic and Taphonomic Context.*—The fossil horizons at Farm Swartpunt preserve a well-studied assemblage of body fossils dominated by erniettomorph taxa, including *Pteridinium simplex*, *Swartpuntia germsi*, *Ernietta plateauensis*, and *Nasepia altae* (Grotzinger et al. 1995; Narbonne et al. 1997; Darroch et al. 2015), along with *Aspidella* and a suite of bilaterian trace fossils (Jensen and Runnegar 2005; Darroch et al. 2015, 2020; Linnemann et al. 2019). Although the community present at Farm Swartpunt is taxonomically diverse by the standards of other fossiliferous sites in the Nama Group, statistical analyses have revealed it to be both less diverse and less complex than similarly preserved communities from the older White Sea- and Avalon-aged assemblages (Darroch et al. 2015, 2018a).

Over three days of fieldwork in 2014, our group performed a survey of the fossil diversity at Farm Swartpunt, recording 104 individual fossils belonging to 5 (potentially 6) genera or form-taxa (see Darroch et al. 2015). Among these were 53 individual *Pteridinium*, over half of which ( $n = 37$ ) were found either in place on the outcrop or could be easily reconstructed back to their original horizons (selected examples shown in Fig. 7). When found in place, several individuals were often seen in close association, with long axes either entirely or approximately aligned (see, e.g., Fig. 7A,F). In

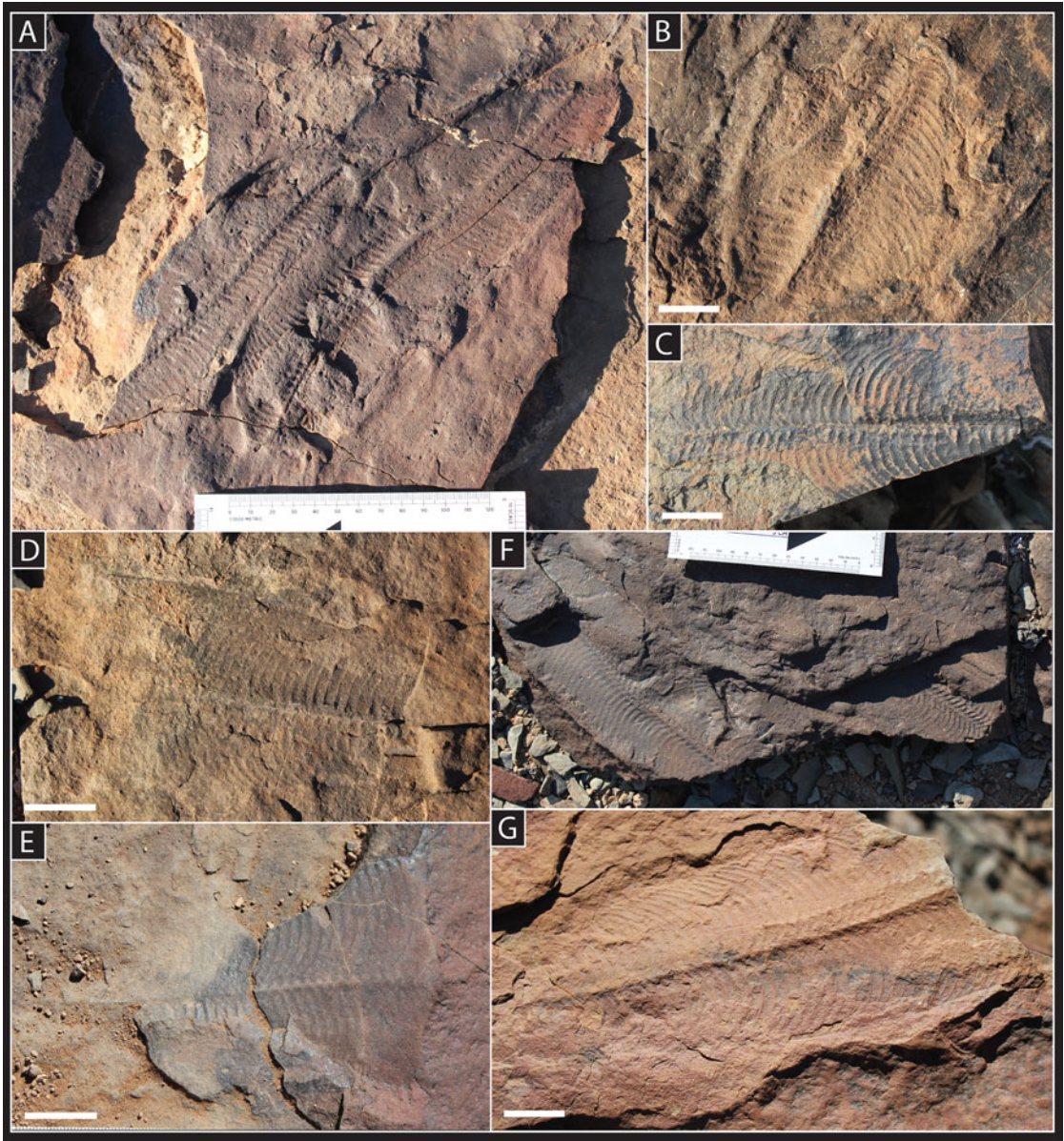


FIGURE 7. A–G, Specimens of *Pteridinium simplex* photographed in the field, from sandstone horizons near the top of the cuesta at Farm Swartpunt (Spitskop Member, Urusis Formation). All fossils in these horizons interpreted as preserved in situ and in approximate life position (see discussions in Narbonne et al. [1997] and Darroch et al. [2015]). Note that all fossils are preserved in two dimensions, in both positive and negative epirelief, and expose lateral vanes with little evidence for a third medial vane. Specimens shown in A–E preserved in situ in the outcrop; G found in float. Scale bars, 2 cm.

terms of the style of preservation, fossil *Pteridinium* from Swartpunt are preserved exclusively in two dimensions on the top surfaces of bedding planes. The central axis and two horizontal vanes are typically visible, commonly missing only the outermost edges, with little or no evidence for a third upright vane. This preservation

of fossils on bed tops in combination with the intact internal stratigraphy of “megaslumped” siliciclastic beds, as well as the lack of any associated evidence for transport of organisms before fossilization, led both Narbonne et al. (1997) and Darroch et al. (2015) to conclude that Ediacara biota at Swartpunt were preserved

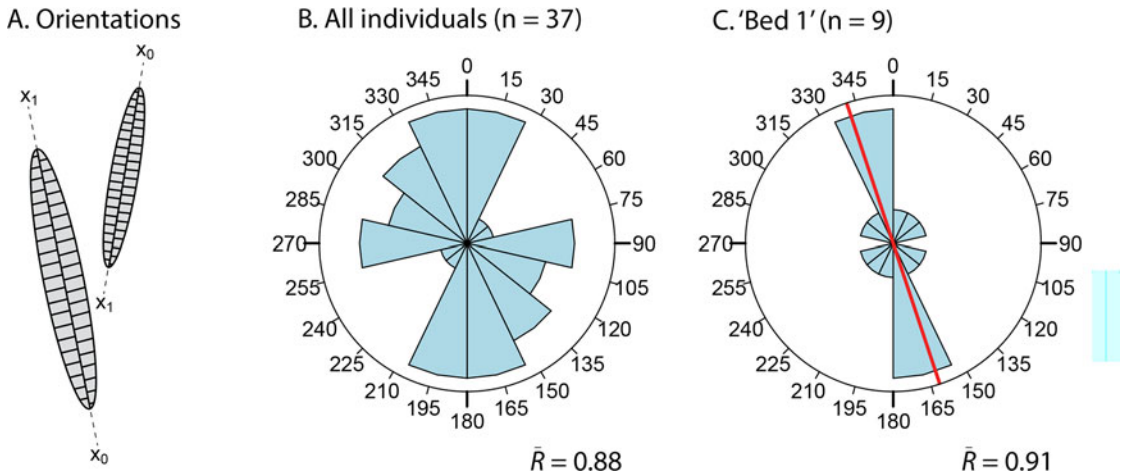


FIGURE 8. Orientations of in situ *Pteridinium simplex* measured in the field from Farm Swartpunt. A, Schematic illustrating orientation measurement; because *Pteridinium* lack anterior–posterior differentiation, each individual has two principal orientations; we defined the first of these directions ( $X_0$ ) as the orientation falling  $0^\circ$ – $180^\circ$  (i.e., easterly), and the second ( $X_1$ ) as the orientations  $180^\circ$ – $360^\circ$  (westerly). B, Orientations for all 37 individual *Pteridinium* found in situ on Farm Swartpunt. C, Orientations for nine individual *Pteridinium* found in situ on a single bed toward the top of the cuesta (Bed 1 of Darroch et al. [2015]; equivalent to Fossil bed A of Narbonne et al. [1997]), along with long-axis orientations of ripple crests (in red) on the same surface. Statistics for B and C give the results of Rayleigh tests, which provide a test for nonuniformity (as unimodal clustering) for compass directions; the  $R$  values (0.88 and 0.91, respectively) suggest a significant preferred alignment. Note that, because *Pteridinium* lacks posterior and anterior differentiation (such that  $0^\circ$  and  $180^\circ$  represent the same orientation), Rayleigh tests are performed on orientation data adjusted to reflect deviation from a fixed compass direction ( $90 - X_0$ ).

largely in situ, rather than transported as part of mass flow deposits (as they are in many other parts of the Witputs Subbasin; see Elliott et al. 2016; Meyer et al. 2014b).

As well as showing local-scale alignment in closely spaced individuals, *Pteridinium* preserved in place at Swartpunt also show a strong overall long-axis alignment, with the majority of individuals apparently oriented NW–SE, and a smaller subset oriented approximately E–W (Fig. 8). A Rayleigh test performed on the long-axis compass directions of these individuals provides equivocal evidence for directionality ( $\bar{R} = 0.56$ ;  $p < 0.01$ ); however, this dataset represents individuals amalgamated over several meters of stratigraphy, and thus any signal of preferred orientation is unlikely. When we restrict our analysis to the orientations of individuals measured from a single bed (Bed 1 of Darroch et al. [2015], equivalent to Bed A of Narbonne et al. [1997]), evidence for a preferred orientation is visually much stronger in the rose diagrams (Fig. 8B), although Rayleigh tests are still equivocal ( $\bar{R} = 0.51$ ;  $p < 0.1$ ). However, because the two ends of the long axis in *Pteridinium* cannot

be given a posterior or anterior assignment (such that  $0^\circ$  and  $180^\circ$  represent the same orientation), we reran Rayleigh tests on orientation data adjusted to reflect deviation from a fixed compass direction (i.e.,  $\text{abs}(90 - x_0)$ ; see Fig. 8A,C). With this adjustment made, Rayleigh tests indicate strong and statistically significant long-axis alignment, in particular for individuals on Bed 1 ( $\bar{R} = 0.91$ ;  $p < 0.01$ ).

Finally, in addition to measuring the long axes of in-place *Pteridinium* on Bed 1, we also measured the long-axis orientation of ripple crests that were found preserved close (i.e., within several meters) to the most densely populated fossil surfaces (Fig. 8C) and from the same bed-top. These ripple crests were oriented  $162^\circ/342^\circ$  suggesting prevailing current flow perpendicular to the long axes of *Pteridinium*.

### Reconstructed Life Habit of *Pteridinium*

Much surrounding the original life position of *Pteridinium* can be inferred through

comparisons with the morphologically similar and coeval taxon *Ernietta*. Both Ivantsov et al. (2016) and Gibson et al. (2019) noted that *Ernietta* from the Kuibis Subgroup in Namibia are overwhelmingly found incompletely preserved, with the bases of fossils (identified via the presence of the basal “seam”) commonly weathering out of outcrops and the upper parts either incompletely preserved or absent altogether. To date, only one individual figured by Ivantsov et al. (2016) from mass-flow deposits on Farm Aar is thought to preserve the complete morphology (illustrating the presence of fluted fan-shaped structures extending up from the top of the organism), suggesting that, in life, the upper parts of the organism were exposed above the sediment–water interface, while the lower parts were buried and thus more readily fossilized. Extending this model to *Pteridinium*, individuals from both the Senckenberg collections and Farm Swartpunt inferred to have been preserved in situ (Figs. 4–5) typically preserve the median axis and the majority of the lateral vanes, missing only the edges of lateral vanes and the upright third vane. By analogy with *Ernietta*, these missing parts of the fossils are likely those that would have been exposed to the water column. Observations from field and museum specimens thus support a recumbent and partially infaunal lifestyle for *Pteridinium* similar to that figured by Meyer et al. (2014a: fig. 2). A key slab in this context is SMF XXX 660i (Fig. 5), which preserves two individuals within a bed of fine-grained sandstone. The two specimens are both aligned and undeformed—inconsistent with transport—but also preserved in three (rather than two) dimensions and within (rather than on top of) the slab. These observations, together with the presence of a fining-up sequence within the bed suggest that these individuals were preserved in life position, albeit in different fashion to either SMF XXX 660q or specimens from Farm Swartpunt. If correct, then the extension of the vanes in both specimens up through the horizon marked by the fining-up sequence would indicate that, in life, the upright third vanes of *Pteridinium* would have extended several centimeters up into the water column.

Aggregated in situ fossils from Namibia suggest that in addition to having a life position partially buried within the sediment, *Pteridinium* lived gregariously. Although our in situ measurements of fossil and current orientations from Farm Swartpunt are limited and need to be tested in other localities (e.g., we note that ripple marks can change from bed top to bottom and are thus hard to interpret in the context of contemporaneous benthic communities), the available data suggest that aggregated *Pteridinium* lived primarily with long axes aligned and approximately perpendicular to prevailing current directions. The absence of any evidence for transport, combined with sedimentological observations indicating low- to moderate-energy paleoenvironments, negates the possibility that individuals were aligned post-mortem. Combined with the inference that certain parts of *Pteridinium* were extended into the water column, this reconstruction implies a relationship between the morphology of *Pteridinium* and the direction(s) of water flow. This reconstruction raises a number of compelling parallels between *Pteridinium* and the similar erniettomorph taxon *Ernietta*; both were sessile, macroscopic organisms that were at least partially buried beneath the sediment–water interface. Furthermore, both extended parts of their anatomy up into the water column where they would have interacted with currents and lived gregariously in aggregated, typically monospecific, communities. This reconstruction therefore also suggests that *Pteridinium* and *Ernietta* possessed similar gross morphologies and supports a close evolutionary relationship.

### Computational Fluid Dynamics

CFD entails numerical simulations of fluid flows and is becoming an increasingly common tool for reconstructing the function and ecology of ancient and enigmatic fossils (Cunningham et al. 2014; Rahman 2017; Gibson et al. 2021b). CFD has proved particularly successful for testing hypotheses pertaining to the biology of the Ediacaran macrobiota (Rahman et al. 2015; Darroch et al. 2017; Gibson et al. 2019; Cracknell et al. 2021), many of which possess unusual body plans that have few counterparts among

modern animal groups, and so have proven difficult to interpret using conventional methods. This approach to Ediacaran paleobiology is founded on the observation that macroscopic organisms living in present-day oceans have evolved a vast array of morphologies that allow them to move, feed, and reproduce in the fluid environment (see, e.g., Vogel 1994). It therefore follows that many of the unusual morphologies exhibited by Ediacaran organisms may plausibly represent similar adaptations. Studies employing this approach have enabled us to develop a robust logic structure with which to interpret reconstructed fluid flow patterns, areas of turbulence, and the distribution of drag forces (Gibson et al. 2021b). This structure allows us to develop specific hypotheses surrounding the influence of *Pteridinium*'s morphology on flow patterns, which we can test using CFD simulations.

*Predictions.*—Among sessile Ediacara biota, the most commonly invoked feeding modes are osmotrophy and filter feeding (Laflamme et al. 2013). The fractal branching of, for example, rangeomorph fronds has been suggested to be ideal for distributing flow evenly over the entire surface of the organism (thus maximizing the potential time and area for uptake of organic matter; see Laflamme et al. 2009; Singer et al. 2012), whereas suspension feeders more often adopt body shapes or attitudes that direct flow to parts of the organism housing specialized feeding structures (summarized in Gibson et al. 2021b). Many Ediacaran taxa—in a similar fashion to extant animals—are inferred to have taken advantage of recirculated downstream flow, which is typically both lower velocity and more turbulent (and thus potentially richer in suspended particles), supporting their interpretation as benthic suspension feeders (Rahman et al. 2015; Cracknell et al. 2021). Gibson et al. (2019, 2021a,b) showed that the erniettomorph taxon *Ernietta* produced low-velocity recirculation within the central cavity of the organism; this was inferred to have led to the settling of food particles and sediment within the cavity (also supported by the presence of laminated sediments within fossil specimens; see Ivantsov et al. 2016), where organic particles could feasibly be sorted and processed by the organism. In addition, Gibson et al. (2019) were able to demonstrate

advantages to *Ernietta* living in aggregated populations; CFD simulations performed on idealized *Ernietta* assemblages revealed a thickening of the turbulent mixing layer above models, providing a mechanism for enhancing nutrient delivery (and availability) to the entire population, while also reducing the waste products funneled into downstream neighbors.

Extending this model to *Pteridinium* allows us to make several testable predictions. Given that we might expect *Ernietta* and *Pteridinium* to have had similar ecologies, we predict: (1) *Pteridinium* created low-velocity recirculation within the central cavity either side of the upright vane. (2) Recirculation within the cavity was maximized when individuals are orientated perpendicular to flow. Finally, because fossil evidence suggests that *Pteridinium*, like *Ernietta*, lived gregariously in aggregated populations, we predict: (3) closely spaced *Pteridinium* individuals produced a thickened turbulent mixing layer above the entire population. Finding evidence confirming these three predictions would support reconstruction of *Pteridinium* as a sessile and gregarious suspension feeder that grew in specific orientations to current. Moreover, this would indicate that the Erniettomorpha as a whole represent a widespread clade of suspension feeders that became common in shallow-marine environments during the latest Ediacaran, potentially reflecting a dramatic diversification in suspension-feeding life strategies (e.g., Wood and Curtis 2014; Cracknell et al. 2021).

*Model Building.*—To test these predictions, we constructed three-dimensional digital models of *Pteridinium* (Fig. 9) using Rhinoceros 3D v. 6. Models were simplified representations of the organism's morphology, which were scaled to the lengths and widths of typical fossil specimens recorded during fieldwork. Due to both uncertainty surrounding the relative height of the central vane and a need to test the effect of specific morphological features on flow patterns, we constructed three idealized models in which we varied key anatomical features. Based on our interpretations of collected and field specimens and published reconstructions (e.g., Meyer et al. 2014a), our base model consists of a hollow half-ellipsoid

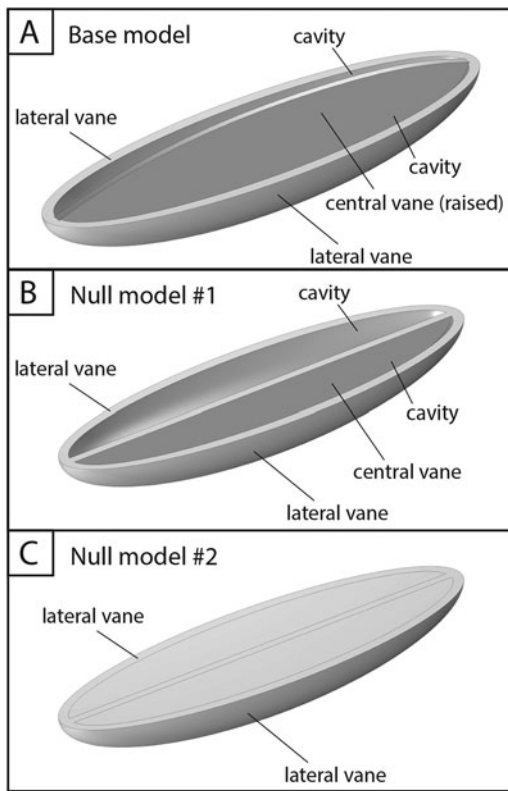


FIGURE 9. Digital model of *Pteridinium simplex*. Construction of our base model (A) and two null models (B, C) for which key morphological features inferred in the fossils have been removed.

with a long-axis medial vane raised above the cavity opening (Fig. 9A). We additionally developed two null models: (1) a hollow half-ellipsoid with a long-axis medial vane flush with the cavity opening (Fig. 9B); and (2) a filled half-ellipsoid without a medial vane (Fig. 9C). Models were exported from Rhinoceros 3D as nonuniform rational B-spline (NURBS) geometries (see Supplementary Models).

*Setup of Fluid Flow Simulations.*—Digital models were imported into COMSOL Multiphysics v. 5.6 for use in computer simulations of fluid flow. We adopted a standardized setup in all our analyses, using a hexahedron (400 × 200 × 40 cm) as the flow domain, with the *Pteridinium* model placed just upstream of the approximate center of the domain (Supplementary Fig. 2). The domain was scaled large enough to ensure that the flow fully developed in both the individual and population-level

simulations (see Gibson et al. 2021a,b). We selected boundary conditions to accommodate a time-dependent analysis using a large eddy simulation (LES) turbulence model. While previous CFD studies of Ediacaran taxa (Rahman et al. 2015; Darroch et al. 2017; Gibson et al. 2019; Cracknell et al. 2021) have relied on stationary solvers using the Reynolds-averaged Navier–Stokes (RANS) shear stress transport turbulence closure, time-dependent LES offers the potential for more accurate simulation of turbulence by not relying on the Reynolds stress tensor (see Gibson et al. 2021b). The upper surface of the flow domain was assigned a slip condition, the lower surface of the domain (i.e., the floor) and all surfaces corresponding to the model of *Pteridinium* were assigned no-slip conditions. All remaining surfaces of the domain were assigned periodic boundary conditions with their respective opposing, parallel surface. A pressure point constraint located on the no-slip lower surface was used as a reference pressure, and a pressure differential (specific to the desired velocity) was applied across the upstream and downstream periodic boundaries to drive flow through the domain (Supplementary Table 1). To determine the pressure differentials for our three desired velocities (see “Simulated Ecological and Environmental Conditions”), we first conducted preliminary stationary analyses of laminar flow with upstream inlet boundary conditions that modeled fully developed flow at the desired velocities and downstream outlet conditions that suppressed backflow. In simulations that were too unsteady (and thus nonlinear) for a laminar flow regime, we used the RANS Spalart–Allmaras turbulence closure because of its ability to quickly approximate flow field conditions (Bardina et al. 1997; Blazek 2001). In all the preliminary CFD simulations, the surfaces of the domain parallel to flow were assigned slip boundary conditions (same as the upper surface), and the lower domain surface and *Pteridinium* model were assigned no-slip boundaries. Using these preliminary solutions, we differenced the absolute averaged pressures across the upstream (inlet) and downstream (outlet) surfaces to determine the necessary pressure to drive flow in our LES analyses. To ensure

that our simulations initialized with physically realistic conditions, thereby minimizing the computation time, we used the preliminary stationary flow field solutions as the initial conditions for our LES analyses. LES simulations were solved with COMSOL's dynamic time-stepping for 30 s of flow time with data outputs at every 0.01 s. Far-field time-averaged velocity ( $U$ ) was plotted to ensure flow fields followed the "law of the wall" (Gibson et al. 2021b). We conducted a mesh sensitivity analysis using the most morphologically complex model (hollow half-ellipsoid with a long-axis medial vane raised above the cavity opening) oriented perpendicular to flow and the highest simulated inlet velocity (0.85 m/s), in which we solved our LES analyses under progressively finer meshes (Supplementary Table 2; using the predefined mesh sizes in COMSOL: "Coarse," "Normal," "Fine", etc.). We then integrated drag forces across the lower, external faces of the *Pteridinium* model at each time step, and time-averaged these values to compare between mesh sizes. Based on this analysis, we selected the Normal predefined mesh size as the best compromise between computational speed and the accuracy of fluid flow results (Supplementary Table 2).

*Simulated Ecological and Environmental Conditions.*—Our paleontological and sedimentological data stemming from descriptions of fossil material, as well as fieldwork in southern Namibia, informed the parameters of our CFD simulations. The effects of any remaining ambiguities in terms of the orientation, burial depth, or precise morphology of *Pteridinium* were tested through the use of different models and/or simulating flow under a range of environmental conditions.

Because of uncertainties surrounding the degree to which *Pteridinium* was buried in life, we simulated two burial depths ("shallow" and "deep"). Given a standard vertical height of 1.5 cm measured from the base of models to the top of the lateral vanes (2.25 cm if the medial vane is included), this results in models in which lateral vanes extend 1.0 and 0.25 cm above the sediment–water interface for shallow and deep models, respectively. We simulate these burial depths for each of the three *Pteridinium* models at two orientations (long axis

oriented parallel or perpendicular to flow), with depth-averaged streamwise flow velocities of  $U = 0.15, 0.50, \text{ and } 0.85 \text{ m/s}$  ( $n = 36$  simulations). These velocities were chosen to reflect the range of currents that have been measured in a range of analogous environmental settings in the present day (see Supplementary Table 3); these measurements were taken using an in situ acoustic Doppler current profiler mounted on an autonomous lander system ~50 cm above the seafloor, which measures velocities in the entire water column layer-wise (i.e., in height "bins") upward to the sea surface. The values shown in Supplementary Table 3 reflect data from the North Sea shelf and the southern German Bight (i.e., shoreface settings) under moderate tide conditions (Klein and Mittelstaedt 1991; Klein and Dick 1999; Klein et al. 1999; Klein 2002).

*CFD Setup for Population-Level Simulations.*—Based on our data suggesting a gregarious life habit for *Pteridinium*, we also performed simulations designed to look at the hydrodynamics of in situ populations consisting of multiple individuals. The boundary conditions and procedures followed the setup used for individual models (see above). Due to the high computational demands associated with simulating flow over multiple individuals, we only tested our median flow velocity (0.5 m/s). Simulations were set up with four individuals in a grid pattern, with all models positioned at a shallow burial depth and with a common long-axis orientation. We carried out two population-level simulations, one with all individuals oriented perpendicular to flow (i.e., the setup that best matches the fossil data), and one with all individuals oriented parallel to flow.

## Results

In this section, we first describe the results of CFD simulations using our base model (i.e., a hollow half-ellipsoid with a long-axis medial vane raised above the cavity opening) oriented perpendicular to flow and at a shallow burial depth, with a flow velocity of 0.50 m/s (Figs. 10–11). This model, orientation, and burial depth best fit our fossil data, while 0.50 m/s represents the median of the three velocities used in our analyses. We subsequently describe

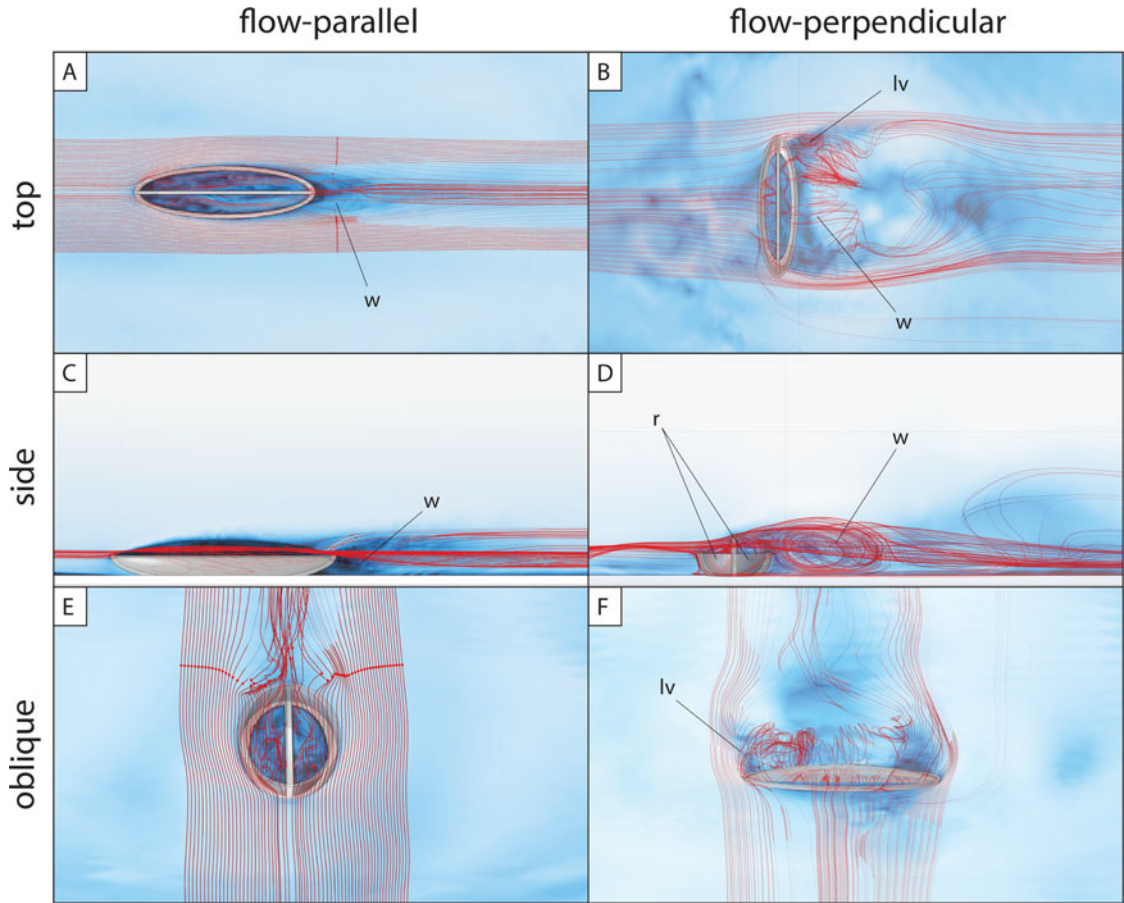


FIGURE 10. A–F, Results of computational fluid dynamics (CFD) simulations using our base model taken as a single frame from time-dependent simulations run at 0.5 cm/s ( $T = 29$  s) (full videos provided in the Supplementary Material). Panels show simulated flow over models in (columns) both flow-parallel and flow-perpendicular orientations and viewed from (rows) top, side, and oblique frontal ( $x, y$ , where flow is moving into the panel away from the field of view) perspectives. Note the wake ( $w$ ) developed in the lee of the model in both orientations. In perpendicular orientation, recirculating flow ( $r$ ) is developed in the cavities, and lateral vortices ( $lv$ ) are occasionally shed off the sides of the model. Flow patterns illustrated by streamlines (in red) overlap of the velocity field ( $U$ ), where the slowest velocities are dark blue, and faster velocities approach white.

the effects of changing orientation, flow velocity, and burial depth, followed by the results for our two null models. Finally, we describe the patterns of fluid flow obtained from the population-level simulations (Fig. 12). Video animations of all simulations are provided in the Supplementary Material on Dryad (<https://doi.org/10.5061/dryad.0rxwdb51g>).

*Individual Model Simulations.*—While we adjusted the parameters described earlier, some flow patterns were ubiquitous within the resulting flow fields. Upstream of the individual model, the boundary layer agrees with that expected from theory, most noticeably in

the observance of the low velocity and laminar viscous sublayer near the no-slip seafloor, which eventually increases velocity and transitions to fully turbulent within the far-field velocity well above the no-slip. As flow approaches the model, it is accelerated around and over the organism model. In general, fluid velocities are markedly slower within the cavity of the organism than outside it. However, our CFD results also reveal complex patterns of relatively low- and high-velocity flow within different parts of the cavity, which are highly sensitive to the simulated life habit (i.e., orientation and burial depth; see below).

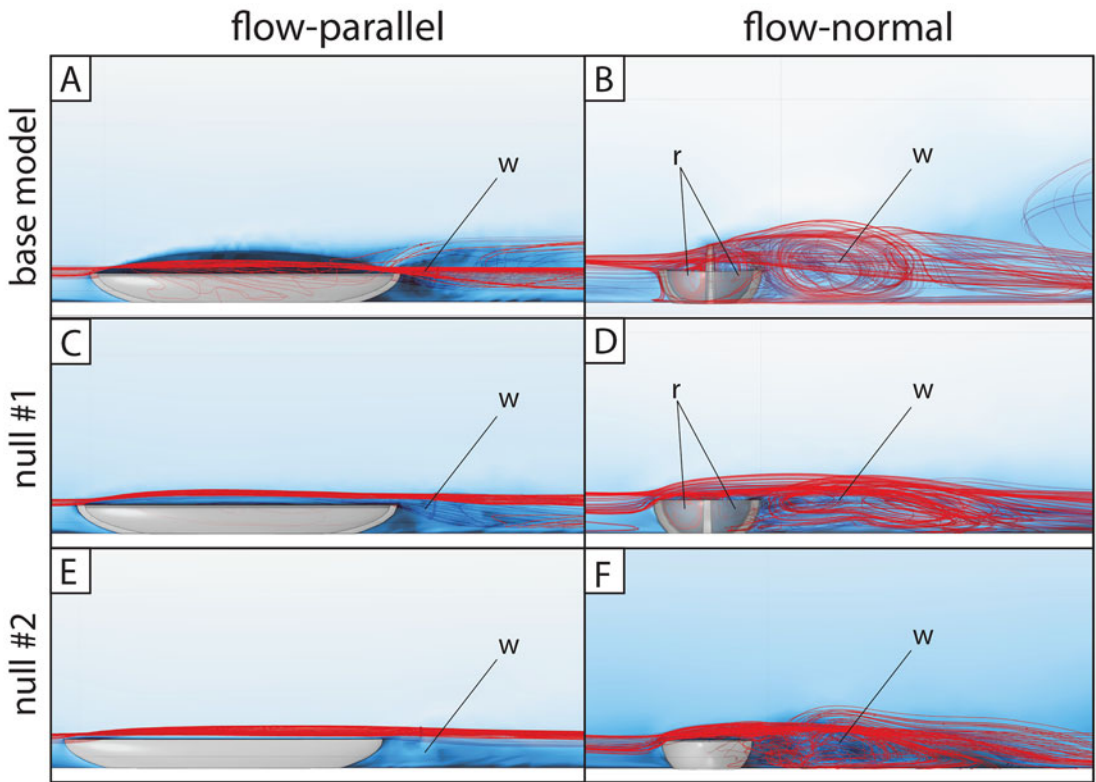


FIGURE 11. A–F, Results of computational fluid dynamics (CFD) simulations taken as a single frame from time-dependent simulations run at 0.5 cm/s (full videos provided in the Supplementary Material). Panels compare simulated flow patterns over our base model (top), null model 1 (middle), and null model 2 (bottom) in both flow-parallel and flow-perpendicular orientations. Wakes (w) and areas of recirculating flow (r) labeled in each panel where appropriate. Note the greater heights of lateral vortices above the sediment–water interface generated in the wake of our base model vs. the two null models and stronger and more consistent recirculation generated within the cavities of our base model. Flow patterns illustrated by streamlines (in red) overlap of the velocity field ( $U$ ), where the slowest velocities are dark blue, and faster velocities approach white.

The model's presence disrupts streamwise flow, creating a turbulent wake downstream, the width and length of which are controlled by model orientation with respect to flow.

*Model Orientation.*—Patterns of fluid flow differ markedly depending on the orientation of the *Pteridinium* model (Fig. 10). In simulations with the long axis perpendicular to flow, fluid is deflected laterally and vertically where it meets the model's leading edge and raised central vane, creating zones of stable and low-velocity recirculation within upstream and downstream regions of the central cavity (Fig. 10B,D,F). Fluid parcels approaching the central vane are deflected to either side, occasionally forming lateral vortices shedding off the lateral margins of the model. An additional

zone of low-velocity recirculation is generated in the downstream region of the cavity behind the raised central vane. A larger zone of low-velocity recirculation is generated downstream of the model (i.e., the wake), characterized by approximately symmetrical vortices.

In the simulations in which the model is oriented parallel to flow (Fig. 10A,C,E), water is deflected up and around the upstream “canoe” face of the model cavity, creating symmetrical regions of low-velocity flow within the cavities on either side of the central vane, which are directed toward the lateral margins (i.e., away from the central vane) in the streamwise direction. Fluid is also directed downward into the cavity and subsequently upward at the downstream raised edge. Additional low-

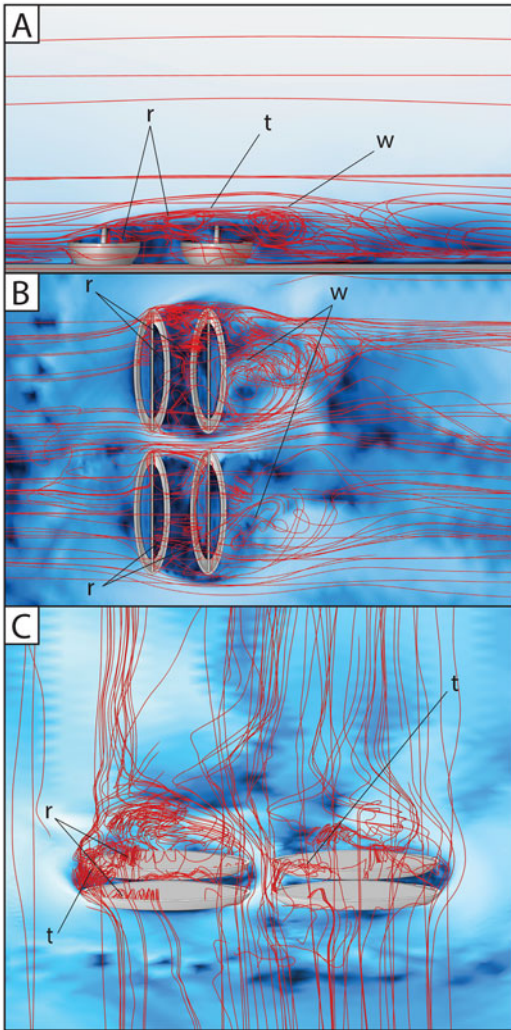


FIGURE 12. A–C, Results of computational fluid dynamics (CFD) simulations using reconstructed populations (as a  $2 \times 2$  array) of our base models in perpendicular orientation, taken as a single frame from time-dependent simulations run at  $0.5 \text{ cm/s}$  (full videos provided in the Supplementary Material). Panels show simulated flow over populations viewed from (rows) top, side, and oblique frontal ( $x,y$ ) perspectives where flow is moving into the panel away from the field of view. Note wake ( $w$ ) developed in the lee of the population, recirculating flow ( $r$ ), both within cavities and in the empty spaces between models, and areas of turbulent flow ( $t$ ) developed above downstream models. Flow patterns illustrated by streamlines (in red) overtop of the velocity field ( $U$ ), where the slowest velocities are dark blue, and faster velocities approach white.

velocity zones are developed adjacent to these high-velocity regions on either side of the central raised vane, as well as in the immediate lee of the model.

*Flow Velocity.*—The broad flow patterns detailed above become stronger and weaker with faster and slower inlet velocities, respectively. With the model oriented perpendicular to flow and an inlet velocity of  $0.85 \text{ m/s}$ , low-velocity zones within the organismal cavity on either side of the raised vane are still present; however, vortices above and behind the organism are asymmetrical and ephemeral (on a second-to-second basis). At an inlet velocity of  $0.15 \text{ m/s}$ , these vortices are more symmetrical and consistently developed. With the model oriented parallel to flow and an inlet velocity of  $0.85 \text{ m/s}$ , both low- and high-velocity regions being generated within the cavity become more pronounced, extending over larger areas. At the same orientation with an inlet velocity of  $0.15 \text{ m/s}$ , high-velocity regions are less well developed, while patches of low-velocity flow either side of the central vane become better developed in the upstream end of the cavity.

*Model Burial Depth.*—In the simulations of a deep burial depth, the exposed rim of the model plays a lesser role in disrupting flow patterns around the organism, with the raised central vane exerting a comparatively greater control on the flow patterns (full videos provided in the Supplementary Material).

With the deeply buried model oriented perpendicular to flow, the raised vane creates low-velocity zones both downstream and (to a lesser extent) upstream of the vane. Additionally, larger areas of recirculation are developed behind the vane and in the wake downstream of the model. Compared with the CFD results of the model placed at a shallow burial depth, there is weaker recirculation in both the upstream and downstream parts of the cavity, a pattern that remains consistent for both faster ( $0.85 \text{ m/s}$ ) and slower ( $0.15 \text{ m/s}$ ) flows. With an inlet velocity of  $0.85 \text{ m/s}$ , there is a greater size disparity between the low-velocity zones either side of the raised vane, with the zone in the downstream part of the cavity more pronounced, and that in the upstream cavity reduced.

With the model oriented parallel to flow and at an inlet velocity of  $0.5 \text{ m/s}$ , the flow patterns observed within the cavity in the more shallowly buried model disappear; flow velocities within and around the organism more closely

approximate far-field boundary layer flow. The remaining low-velocity zones are concentrated adjacent to and immediately downstream of the central vane, while there remains some turbulence above and downstream of the model where flow split by the raised vane reattaches. The low-velocity zone behind the central vane is enlarged at an inlet velocity of 0.85 m/s, whereas it is reduced at an inlet velocity of 0.15 m/s. Otherwise, most features of the flow are conserved across the different inlet velocities.

*Null Models.*—We carried out simulations of two null models to test how a medial vane raised into the water column and a central organismal cavity, respectively, affect fluid flow patterns (Fig. 11).

With an orientation perpendicular to flow (shallow burial depth; inlet velocity of 0.5 m/s), our first null model—a hollow half-ellipsoid with long-axis medial vane flush with cavity opening—deflects fluid around and upward, where it meets the raised edge of the model, generating pronounced low-velocity zones in the central cavity either side of the medial vane, as well as in the downstream wake (Fig. 11D). Some zones of recirculation are generated inside the cavity either side of the medial vane, although these are smaller and more ephemeral compared with those observed for the base model in the same orientation (Fig. 11B). Large, lateral vortices of turbulent flow are generated in the wake of the null model, which are again smaller than those generated with our base model, and are restricted to shorter distances above the sediment–water interface. Patterns are again conserved but scale with faster/slower inlet velocities (full videos provided in the Supplementary Material); at an inlet velocity of 0.15 m/s, recirculation in the central cavity downstream of the medial vane largely vanishes, leaving a stagnant zone—something not seen in our base model under the same conditions. With the same model oriented parallel to flow, fluid is deflected to either side of the model, generating low-velocity zones within the central cavity and in the wake (Fig. 11C). The principal differences from the base model (Fig. 11A) are that this null model (Fig. 11C) generates a smaller wake, which extends to a lower height above the sediment–water interface. These

differences are enhanced at faster inlet velocities of 0.85 m/s and muted at lower inlet velocities of 0.15 m/s. With deeper burial, these general patterns become even more muted, such that models cause comparatively little disruption of flow throughout the velocity field.

In simulations of the second null model—a filled half-ellipsoid oriented perpendicular to flow (shallow burial depth; inlet velocity of 0.5 m/s)—fluid is deflected above and around the model (Fig. 11F). The wake is restricted to much lower heights above the sediment surface than in simulations of the base model at all simulated velocities. These broad patterns are strengthened/weakened at inlet velocities of 0.85 m/s and 0.15 m/s (full videos provided in the Supplementary Material), respectively, but inlet velocity does not greatly influence the height of the wake. In a deeper burial position and perpendicular to flow, the model mostly sits within the viscous boundary layer and so generates only minor turbulent features; there is a small wake developed behind the model, but little downstream recirculation or lateral deflection. There are few changes at 0.15 m/s, while relatively small vortices are shed downstream at the fastest simulated velocities (0.85 m/s). Oriented parallel to flow, the deeper-buried model generates comparatively little turbulence beyond a small wake. Increasing or decreasing the simulated velocity has little effect on these overall patterns (see Supplementary Material).

*Community Simulations.*—With models oriented perpendicular to flow, hydrodynamic patterns over and around aggregated *Pteridinium* show some key differences compared with those seen in individual models (Fig. 12). First, although the strength and pattern of recirculation within the upstream models are similar to those in the simulations of individuals, fluid recirculation is much stronger and more consistent in the cavities of downstream individuals—particularly on the upstream side of the vanes. Second, the disparity in fluid velocities between upstream and downstream faces seen either side of the raised vane in the individual models largely disappears, such that downstream individuals experience similar overall velocities either side of the raised vane. Third, the presence of upstream individuals creates

increased turbulence above downstream individuals. Fourth, population-level simulations illustrate the generation of vortex shedding and thus greater turbulence downstream of individuals and, moreover, turbulence that reaches a greater height above the sediment–water interface than seen in the individual models. Finally, a feature of population-level simulations in this orientation not seen in individual models—in addition to strengthened recirculation within organismal cavities—is the generation of recirculating fluid between rows of individuals.

Oriented parallel to flow, hydrodynamic patterns also show some key differences to those seen in individual models. Principally, flow enters the cavities of upstream models and is deflected upward, where it meets the downstream raised edge (much as it is in individual model simulations). However, this leads to less fluid entering the cavities of downstream individuals, thus creating a strong overall velocity disparity in the cavities of upstream versus downstream models. Other aspects of the flow patterns are consistent with those seen in the individual simulations (e.g., symmetrical patches of low-velocity flow either side of the central vane) but are strongly developed in upstream models and weakly developed in downstream models. There is little recirculation within the cavities of either upstream or downstream models, and no evidence for recirculating flow in the space between organisms (as there is in perpendicular orientation).

## Discussion

The CFD results support our initial hypothesis that *Pteridinium* could have functioned as a suspension feeder, but demonstrate that this lifestyle was contingent on a number of paleobiological and paleoecological factors. In the following sections, we discuss how patterns of fluid flow around *Pteridinium* models might have aided feeding and evaluate the role of specific anatomical characters in either creating or strengthening these patterns. Based on this evaluation, we suggest some possible roles that *Pteridinium* may have played in latest Ediacaran benthic communities. Finally, we discuss uncertainties arising from this reconstruction

and consider some alternative hypotheses that may also be consistent with the paleobiological and environmental data presented here.

*Pteridinium as a Suspension Feeder.*—Using *Ernietta* as an interpretative model (see Ivantsov et al. 2016; Gibson et al. 2019), we predicted that the morphology of *Pteridinium* would create areas of relatively low-velocity and recirculating flow that would have led to the settling of suspended sediment and food particles over specific regions of the organism, where they could (presumably) be processed and ingested. The results of our CFD simulations demonstrate that low-velocity recirculation is generated in the cavity of *Pteridinium* models either side of the central vane—analogue to the central cavity in *Ernietta*—at a wide range of modeled flow velocities (prediction 1). However, critically, these flow patterns are only generated when the long axes of the models are aligned perpendicular to current. With the models oriented parallel to flow, fluid velocity decreases upon entering the cavity, but there is no evidence of recirculation similar to that observed in *Ernietta*, which would have played an important role in increasing the opportunity for food particles to settle and/or be captured (Gibson et al. 2019). Moreover, at higher flow velocities, we see that the local fluid velocities in the cavity and in the immediate vicinity of the model noticeably increase, which would likely have led to scouring (rather than deposition) of material inside the cavity. This scouring would likely have removed any food particles, thereby limiting opportunities for uptake of nutrients, and moreover is not something suggested by the sedimentology in and around the actual fossils. In contrast, with the model perpendicular to flow, our simulations illustrate the development of consistent lateral vortices within the cavities on either side of the raised vane at all simulated inlet velocities, suggesting that *Pteridinium* would have created flow patterns conducive to suspension feeding under a wide range of realistic environmental conditions (prediction 2).

These inferences provide an intuitive match with our field and specimen data, which suggest that populations of *Pteridinium* were preferentially oriented with their long axes aligned approximately perpendicular to the

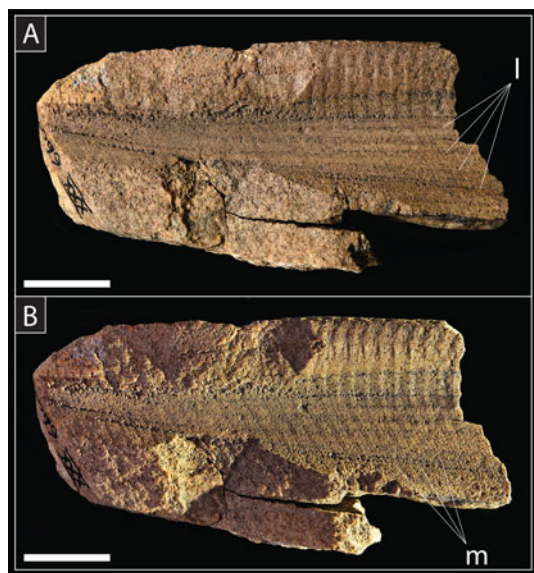


FIGURE 13. SMF XXX 660c; preserving the upright vane of a single *Pteridinium simplex* exposed in cross section in the side of the slab. Panels illustrate specimen lit from two angles to illustrate: A, millimeter-scale laminae (l) within the slab; and B, the outline of individual modules (m) running down through cross-bedded laminae, illustrating the sediment was accumulating within the cavity of the organism during life. Scale bars, 2 cm.

prevailing current direction (Fig. 8). In this orientation, stable vortices of recirculating flow would have been generated in cavities either side of the central vane, which would have led to the settling of both sediment and suspended food particles in cavities, similar to the coeval taxon *Ernietta* (Gibson et al. 2019). Interestingly, support for our first prediction might also imply that that layered sediment would be forming inside the cavities of *Pteridinium* in life (see, e.g., Ivantsov et al. 2016). To a large extent, this is borne out by close observation of slab SMF XXX 660i (Fig. 5), which preserves two specimens inferred to be in life position and with at least two episodes of deposition recorded in the sediments filling the cavities. In addition, close examination of slab SMF XXX 660c (Fig. 13) reveals millimeter-scale bedding within the exposed cavity of the specimen, providing strong evidence indicating the sediment was accumulating in the cavity during life. In the vast majority of the material housed at Senckenberg, however, internal sediments consist of metamorphosed quartzites preserving no internal

structure, and so the extent to which internal layered sediments are ubiquitous is not known. The presence of sedimentary laminae within cavities is, therefore, something that should be examined in other specimens and may reveal much about patterns of fluid flow in and around *Pteridinium* during life.

*Anatomical and Paleobiological Constraints from Null Models.*—Our CFD simulations using two null models and varying model burial depth provide additional information about the roles of specific anatomical features in generating flow patterns conducive to suspension feeding.

Contrasting results for the second null model (filled half-ellipsoid) oriented parallel and perpendicular to flow at shallow burial depth (Figs. 9C, 11E,F) illustrate that, in the absence of any other external morphology, organisms oriented perpendicular to flow generate stronger interactions with moving fluids and are far more conducive to generating patterns of recirculation around specific parts of the organism. Building on this, contrasting flow patterns around the base model with our first null model (hollow half-ellipsoid with long-axis medial vane flush with cavity opening) oriented perpendicular to flow (Figs. 9B, 11C,D) highlight the importance of a raised central vane in forming stable and recirculating lateral vortices within the cavity of *Pteridinium*. Our simulations illustrate that, while weaker and less consistent than in the base model (especially in the downstream part of the cavity), recirculating vortices are still developed within the cavity of the first null model. This suggests that a central vane raised up into the water column (rather than flush with the edges of the lateral vanes) would have been conducive to, but was not strictly necessary for, the generation of flow patterns thought to aid in suspension feeding. Additionally, the presence of a raised central vane creates vortex shedding at much greater heights in the water column and thus would ensure a more reliable source of well-mixed fluid (and thus, by extension, suspended food particles) to downstream neighbors.

In contrast, our simulations varying burial depth reveal more substantive barriers to the formation of recirculating flow within the cavity; in a deeper burial position, there is little

to no recirculation in either the base or null models (although flow in these areas is still substantially slowed). This indicates that, if *Pteridinium* was indeed functioning as a benthic suspension feeder relying on the settling of food particles in the central cavity, there would have been a definite advantage to having both central and lateral vanes extended above the sediment–water interface and above the height of the viscous sublayer. We argue that the biostratigraphic and sedimentological evidence preserved in slab SMF XXX 660i (Fig. 5) indicates that, in life, the central vane of *Pteridinium* was likely raised at least several centimeters into the water column, consistent with our modeled shallow burial depth. Thus, the simulated ecological conditions best supported by our fossil data (i.e., specimens oriented perpendicular to current at a shallow burial depth) are most consistent with the inference of a suspension-feeding lifestyle for *Pteridinium*.

*Evidence for Ecological Facilitation.*—Our population-level simulations suggest that, when closely spaced and with a common orientation perpendicular to flow (as suggested by the fossil data), in situ populations of *Pteridinium* would have created flow patterns in downstream individuals that were especially conducive to the settling of food particles within cavities (Fig. 12), revealing a potential advantage to feeding in aggregations (similar to the closely related erniettomorph *Ernietta*; see Gibson et al. 2019, 2021a,b). In addition, CFD results indicate the presence of increased turbulence above downstream individuals (prediction 3). This turbulent flow could have aided suspension feeding by enhancing delivery of nutrients to downstream individuals and remixing (presumably nutrient-depleted) fluid sourced from the cavities of upstream individuals with more nutrient-rich ambient flow, serving both to disperse waste products and prevent nutrient depletion downstream. These hydrodynamic phenomena and their benefits in context of feeding in aggregated benthic populations have been described for modern marine taxa (see, e.g., Smits and Wood 1985; Butman et al. 1994). Therefore, our results suggest that populations of *Pteridinium*, similar to *Ernietta*, represent an ancient example of

ecological facilitation, reinforcing the point that—even though there is little evidence to unambiguously link erniettomorphs with animals—their community structure and ecological interactions show at least some similarities to those formed by metazoans (see also Clapham et al. 2003; Gibson et al. 2019, 2021a,b).

*Community Reconstruction.*—On the basis of evidence stemming from redescribed fossil material, field observations, and CFD simulations, we infer that *Pteridinium* was a gregarious suspension feeder that formed aggregated populations in a range of late Ediacaran marine environments ~555–539 Ma. The fossil material supports reconstructing *Pteridinium* as a three-vaned canoe-shaped organism in which all three vanes met along a seam, with their distal tips extending above the sediment–water interface. When oriented perpendicular to the direction of the prevailing current, the morphology of *Pteridinium* would have created stable vortices of low-velocity recirculating flow inside the cavities on either side of the central vane; this would have led to the settling of food particles inside the organism. These patterns would have been enhanced if—as suggested by the fossil data—the central vane was raised into the water column above the height of the lateral vanes; however, our first null model demonstrates that suspension feeding would still have been plausible if the vane was flush with the cavity opening. In aggregations with long axes aligned, this morphology would have served to further increase mixing within clustered populations, thus enhancing the transport of suspended food particles to downstream neighbors (as inferred for *Ernietta*; see Gibson et al. 2019). This arrangement may have created competition for food in downstream individuals but could have been compensated for under tidal conditions when flow was bidirectional.

Because these flow patterns are reliant on orientation to current (and *Pteridinium* was almost certainly sessile), our results might imply that *Pteridinium* was likely restricted to environments characterized by overwhelmingly unidirectional (or, more likely, bidirectional) current directions. This stands in contrast to *Ernietta*, whose morphology produces flow patterns that would have aided in

feeding in all orientations (Gibson et al. 2019, 2021a) and thus may have been better suited to environments characterized by variable or multidirectional currents (see also discussion surrounding *Tribrachidium* in Rahman et al. [2015]). In support of this, in southern Namibia at least, the existence of bidirectional currents is plausible, principally because paleogeographic reconstructions for the late Ediacaran (see, e.g., Meert and Lieberman 2008) place the Nama region as part of a relatively shallow-water coastal environment at the margin of the Kalahari craton directly facing the ocean. In equivalent environments in the present day, these settings are typically subject to semidiurnal tides with a mesotidal range—conditions that frequently create bidirectional currents. Given that *Pteridinium* and *Ernietta* are only rarely found together in in situ communities, this may also suggest a degree of niche partitioning, with each taxon possessing morphological adaptations to living in parts of the shallow shelf influenced by different current regimes (or alternatively, selective ability in recruitment abilities). Further detailed investigation of fossil communities and sedimentary structures along shelf profiles (especially in the Nama Group) could serve as a robust test of this hypothesis.

Reconstructing *Pteridinium* as a sessile and gregarious suspension feeder adds to the growing number of inferred suspension feeders in the late Ediacaran, at the expense of taxa previously thought to have been osmotrophic (Xiao and Laflamme 2009; Laflamme et al. 2013). In turn, this may be emblematic of a broader paleoecological shift toward benthic suspension-feeding strategies over the course of the latest Ediacaran. Although many taxa belonging to the Avalon interval (~571–558 Ma) are still thought to have fed osmotrophically (Sperling et al. 2011; but see Butterfield 2020), by the White Sea interval (~558–550 Ma) there was a marked increase in taxa inferred to have functioned as suspension feeders, in particular those occupying low tiering heights above the sediment–water interface (Rahman et al. 2015; Darroch et al. 2017; Cracknell et al. 2021). By the latest Ediacaran Nama interval (~550–539 Ma), suspension feeding had apparently spread to a wide variety of other niches and paleoenvironmental settings,

including higher tiering levels (Pacheco et al. 2015), reef tops (Penny et al. 2014; Shore et al. 2021), and cryptic habitats (Wood et al. 2002). Given that suspension feeding represents a crucial link between the pelagic and benthic ecosystems (increasing rates of energy transport from the water column to the sediment surface; see, e.g., Wood and Curtis 2014), a proliferation in suspension feeders could plausibly have helped to fuel the Cambrian explosion (Lerosey-Aubril and Pates 2018; Cracknell et al. 2021). We concede that the paleobiology of many White Sea-aged Ediacaran taxa are still unknown, and thus the notion of late Ediacaran “rise of suspension feeding” remains hypothetical. Studies focused on individual taxa and employing CFD do, however, offer a means for testing this hypothesis and promise to shed new light on the roles played by new metazoan feeding modes in driving waves of evolutionary innovation over the Ediacaran/Cambrian transition.

*Outstanding Questions.*—Despite the evidence for our reconstruction of *Pteridinium* stemming from fossil material and computer simulations, there are several outstanding questions surrounding how the organism could have plausibly functioned as a suspension feeder, and the relationships of *Ernietta* to extant metazoan clades.

In terms of the first question, although there is an abundance of evidence to suggest both that sediment would have settled into the central cavities of *Pteridinium* and *Ernietta* during life (Ivantsov et al. 2016) and that there was a ready supply of food for benthic suspension feeders (see, e.g., Bobrovskiy et al. 2020), it is unclear how these food particles might subsequently have been captured and processed by the organisms. Strategies for suspension feeding were categorized by LaBarbera (1984) into six broad categories: (1) “scan and trap,” (2) sieving, (3) direct interception, (4) inertial impaction, (5) gravitational deposition, and (6) diffusive deposition. Of these, the feeding mechanism we infer for both *Pteridinium* and *Ernietta* is closest to gravitational deposition, whereby gravity causes the suspended particles to cross streamlines and fall onto a collecting apparatus—something that can intuitively be achieved by either slowing or reducing the turbulence of the host fluid (see, e.g., Bernard

1974). Gravitational deposition is also a mechanism that has been inferred for other putative Ediacaran suspension feeders (see, e.g., Rahman et al. 2015; Cracknell et al. 2021), however, while these taxa possess distinctive anatomical features into which material would have settled and thus may plausibly represent sites of particle collection (see, e.g., the “apical pits” of *Tribrachidium*), there are no such anatomically distinct sites within the cavities of *Pteridinium* or *Ernietta*. Of the few extant organisms definitively shown to use gravitational deposition as a means of suspension feeding, most also possess a mechanism for separating food particles from inorganic sediment (see, e.g., the Pacific oyster *Crassostrea gigas*; Bernard 1974), such that food is preferentially passed to the mouth and ingested, while the rest is rejected as pseudofeces. There is, however, no fossil or sedimentological evidence to suggest that either *Pteridinium* or *Ernietta* were actively sorting the particulate material settling into their central cavities. Given sufficient density contrasts between organic and inorganic material, it is plausible that cilia located on either side of the central vane could have captured food particles suspended in intracavity slowly circulating flow, but evidence for these would stand little/no chance of being preserved in the fossils. Moreover, there is no evidence among any of the Erniettomorpha for a gut system where food could ultimately be processed. Still more problems emerge when one considers the frondose taxon *Swartpuntia*; while undoubtedly an erniettomorph (Laflamme et al. 2013; Decechi et al. 2017), it possesses no cavities into which material might settle, and thus it is unclear how it could have fed in analogous fashion (however, we note that in the absence of a model of homology between erniettomorph taxa against which to test functional hypotheses, we cannot currently say further). Similar issues emerge when considering the White Sea-aged strap-like taxon *Phyllozoon*, which was recently reinterpreted as an erniettomorph by Gehling and Runnegar (2021) and apparently lived entirely recumbent on the seafloor. Thus, while the morphologies of erniettomorphs such as *Pteridinium* and *Ernietta* seem well adapted for creating flow patterns that would be conducive to suspension feeding, it

seems unlikely that this behavior was distributed across all Erniettomorpha, nor are there easy comparisons to be made to extant metazoans.

Leading into the second question, one possible reconstruction that does not rely on feeding via gravitational deposition (but which would nonetheless benefit from the modeled flow patterns), revolves around reconstructing erniettomorphs as colonial organisms. This interpretation of soft-bodied Ediacara biota is not new. Glaessner (1959a,b) interpreted several frondose forms as representing octocorallian Anthozoa, while Jenkins (1985) interpreted *Rangaea* as comprising a large number of feeding polyps—pointing to the highly ordered and complex character of rangeomorph petaloids. Buss and Seilacher (1994) noted that the “quilted” construction of erniettomorphs resembled a series of polyps lacking oral openings and further hypothesized that erniettomorphs represent ancestral cnidarians that fed via a symbiotic association with either photosynthetic or chemosynthetic bacteria (thus explaining the lack of a mouth). Although we make no specific claims for where erniettomorphs may sit on the metazoan tree (or whether they represent metazoans at all), we do suggest that many of the characteristics of erniettomorphs would also make sense if, rather than a single organism, they represented colonial or modular organisms in which each tube hosted an individual. This reconstruction would, for example, be compatible with many of the flow patterns associated with both *Pteridinium* and *Ernietta* (recirculation within cavities would bring suspended food particles into close proximity to the distal ends of modules, where feeding structures presumably would be hosted) and would also explain why the frondose erniettomorph *Swartpuntia* lacks any obvious mechanism for capturing food and/or sediment similar to that suggested for *Pteridinium* and *Ernietta* (the tubes that make up the petaloids of *Swartpuntia* could likewise have hosted individual organisms—albeit suspended higher above the sediment–water interface). In addition, it would be consistent with the pattern and apparent indeterminate growth exhibited by many erniettomorphs; increasing size in erniettomorphs was achieved by the addition of new units of consistent width with

growth (Grazhdankin and Seilacher 2002; Laflamme et al. 2009), and there does not appear to be a fixed upper limit on how large erniettomorphs such as *Pteridinium* could get.

Finally, a colonial reconstruction would also be broadly consistent with some features of the tubular modules in erniettomorphs that have long puzzled paleontologists—specifically, that the basal ends of modules (i.e., those closest to the seam joining all three vanes) appear to have been actively packed with sediment during life, while the distal ends appeared to have been left open and (potentially) fluid filled (Droser et al. 2006; Seilacher and Gishlick 2014; Ivantsov et al. 2016). Ivantsov et al. (2016) noted that the lithology and diagenesis of sand-filled modules did not match the host sediment, implying that sediment was incorporated into the modules before transport, death, and burial. These observations would make some sense if individual organisms within the colony were living in the distal ends of modules where they had access to the water column and packing sediment behind them as a means for strengthening the overall colony structure (much like some colonial sea anemones and sponges do; see, e.g., Schönberg 2016). One problem with this model is that authors disagree on whether the distal tips of modules were open or closed. Droser et al. (2006) noted that preserved modules in *Pteridinium* from the Spitskop Member (Nama Group, Namibia) were open at the distal ends, while Ivantsov et al. (2016) suggested that Aar Member individuals were preserved with modules closed. Open modules would explain the sediment accumulation seen in three-dimensional specimens, while closed modules would make this observation problematic and also preclude the possibility that individual organisms could feed out of them. Given reports of both open and closed modules, it is possible there were originally thin, soft-tissue structures present that allowed opening and closing of modules, which have not been preserved in the fossils. It is possible that the variation seen in the distal termination of different species of *Pteridinium* (e.g., rounded globular termination of *P. simplex* vs. the sharper terminations seen in the likely junior synonym *P. nenoxa* [formerly *Onegia nenoxa*]; Keller et al. 1974) could represent a

taphonomic expression of the extent of sediment filling the modular units, thus supporting their current synonymy.

The described anatomy of *Pteridinium* is therefore compatible with its functioning as a modular organism in which tubes are discrete entities that grow together (as in, e.g., living sponges), but whether or not *Pteridinium*—and other erniettomorphs—were colonial organisms requires further investigation. The consistent and predictable relationship between module length and number (e.g., Grazhdankin and Seilacher 2002) is unlike growth strategies typically employed by colonial animals, which tend to show variation in individual polyp/module size or colony form, and implies a centralized program of growth observed in only the most tightly integrated and highly derived colonial animals (e.g., siphonophore cnidarians). Furthermore, in the absence of information on the earliest stages of morphogenesis, we do not yet know how these modules differentiated from one another; if modules derived ultimately from a single, primary module (as is the case with some other classical Ediacaran macrofossils; Dunn et al. 2021), then a colonial arrangement would not be likely, but if modules derived sequentially or simultaneously from a shared basal structure, these data may support the colonial hypothesis. Additionally, recent work by Gehling and Runnegar (2021) has suggested that the gregarious, recumbent form *Phyllozoon* may be closely related to *Pteridinium* and can be considered an erniettomorph. *Phyllozoon* appears to show evidence of modules merging distally, which would not be compatible with our suggestion of a colonial arrangement for *Pteridinium*. However, the affinities of *Phyllozoon* remain to be tested in a phylogenetic systematic framework.

In the absence of obvious anatomical markers of affinity, establishing the life history of *Pteridinium* is critical, because a multicellular and colonial life habit would support an animal affinity to the exclusion of other hypotheses and so offers a chance at finding a home for erniettomorphs in the tree of life.

## Conclusions

Detailed redescription and reexamination of *Pteridinium simplex* specimens housed at

the Senckenberg Forschungsinstitut und Naturmuseum Frankfurt, in combination with field observations of fossiliferous surfaces in southern Namibia, support interpretation of this taxon as a three-vaned, canoe-shaped eukaryote that lived semi-infaunally within aggregated populations and with long axes preferentially oriented perpendicular to current. Following from this reconstruction, CFD modeling illustrates that this morphology and life habit would have created stable vortices of low-velocity recirculating flow inside the cavities on either side of the central vane; this would have led to the settling of food particles inside the organism and thus supports reconstructing *Pteridinium* as a late Ediacaran benthic suspension feeder that functioned similarly to the coeval taxon *Ernietta plateauensis*. Crucially, modeled flow patterns also predict the accumulation of layered sediments within the cavity of *Pteridinium* during life—a prediction confirmed following close examination of the fossil material. This study adds to the growing number of inferred suspension feeders in the late Ediacaran, which may be emblematic of a broader paleoecological shift toward benthic suspension-feeding strategies over the course of the latest Ediacaran. Finally, despite the new evidence presented here, we note that there remain a number of outstanding paleobiological questions surrounding how erniettomorph taxa such as *Pteridinium* and *Ernietta* may have fed—specifically, how they subsequently ingested and processed food particles. Although some of these questions could be satisfied via reconstructing these taxa as colonial organisms, this reconstruction receives equivocal support from the available (albeit sparse) developmental data. Thus, although there is still little evidence to ally erniettomorphs such as *Pteridinium* with any extant metazoan groups, our new data and reconstruction generate hypotheses that can be tested via detailed analysis of erniettomorph growth and development.

### Acknowledgments

All authors are profoundly grateful to M. Ricker (Senckenberg, Frankfurt) for providing photographs of the Senckenberg material,

as well as making both polished and thin sections. This research was supported by joint funding from the National Science Foundation (NSF-NERC EAR-2007928) and Natural Environment Research Council (NE/V010859/2) to S.A.F.D., I.A.R., F.S.D., and R.A.R. Fieldwork in Namibia was supported by a National Geographic grant (no. 9968-16) to S.A.F.D and M.L. and an NSERC Discovery grant (RGPIN 435402) to M.L. S.A.F.D. and R.A.R. also acknowledge generous support from the Alexander von Humboldt Foundation, which is sponsored by the Federal Ministry for Education and Research in Germany. B.M.G. was funded by a University of Toronto Mississauga Postdoctoral Fellowship and acknowledges computational support stemming from two Vanderbilt University Alberstadt, Reeseman, and Sterns grants. F.S.D. acknowledges additional support from the Royal Commission for the Exhibition of 1851 and Merton College, Oxford. This article was considerably improved after constructive reviews from S. Evans and an anonymous reviewer.

### Data Availability Statement

Data available from the Dryad Digital Repository: <https://doi.org/10.5061/dryad.0rxwdb51g>.

*Supplementary Models.*—Our base model and two null models (1: hollow half-ellipsoid with a long-axis medial vane flush with the cavity opening; and 2: filled half-ellipsoid without a medial vane), exported from Rhinoceros 3D as nonuniform rational B-spline (NURBS) geometries.

*Additional raw data files.*—COMSOL simulation files giving the set-up of simulations for our *Pteridinium* simplex base model and two null models, along with the set up for population-level simulations are stored on a Microsoft Sharepoint site found here: [https://vanderbilt365.sharepoint.com/:f:/s/Ediacaranfluidynamics/EubZLTVa\\_9BrzRNLt1wOOQBIDpCh9n1KFOUX5W4XIUHdg?e=8ngDAi](https://vanderbilt365.sharepoint.com/:f:/s/Ediacaranfluidynamics/EubZLTVa_9BrzRNLt1wOOQBIDpCh9n1KFOUX5W4XIUHdg?e=8ngDAi).

Supplementary information available on the Zenodo Digital Repository: <https://doi.org/10.5281/zenodo.6415297>

*Supplementary Figure 1.*—Locality and stratigraphy information, modified from Darroch

et al. (2020): A, map of the Nama Group south of Windhoek, showing the locations of the Zaris (ZS) and Witputs (WS) Subbasins (separated by the Osis Arch), along with (numbered) localities that preserve Ediacaran–Cambrian body and trace fossils. The *Pteridinium* fossils investigated as part of this work come from the Witputs Subbasin, from Farm Aar (locality no. 15, upper Kli-phoek Member, Dabis Fm.) and Farm Swartpunt (locality no. 17, Spitskop Member, Urusis Fm.)—both starred. For details of other localities, see Darroch et al. (2020). B, Generalized stratigraphy of the Witputs Subbasin with the *Pteridinium*-bearing horizons highlighted in A indicated; geochronological dates after Linne-mann et al. (2019).

**Supplementary Figure 2.**—Generalized setup for all computational fluid dynamics (CFD) simulations. Boundary conditions for stationary, initial simulations are in unformatted font, while boundary conditions specific to the time-dependent large eddy simulation are labeled in bold.

**Supplementary Table 1.**—Pressure differentials used to create fast, intermediate, and slow current velocities ( $U = 0.85$  m/s, 0.5 m/s, and 0.15 m/s, respectively) in computational fluid dynamics (CFD) simulations.

**Supplementary Table 2.**—Mesh sensitivity analyses performed using COMSOL's automated meshing (“Finer,” “Coarser,” etc.). Drag was integrated across external model faces in each simulation. With increasing discretization, drag value convergence also increased. From Coarse to Normal yielded 16% absolute difference, which was sufficient to observe macroscopic flow patterns without the added computational time required for increased mesh resolution. Total simulation time for all 38 simulations (e.g., simulations excluding sensitivity analyses) was >1000 hours, making finer mesh sizes (i.e., greater mesh discretization) unfeasible.

**Supplementary Table 3.**—Current velocities measured in a range of shallow-marine shore-face settings in the North Sea shelf and southern German Bight (compiled from Klein and Mittelstaedt 1991; Klein and Dick 1999; Klein et al. 1999; Klein 2002). Measurements taken using an in situ acoustic doppler current profiler mounted on an autonomous lander system ~50 cm above the seafloor, which

measures velocities in the entire water column layer-wise (i.e., in height “bins”) upward to the sea surface.

**Supplementary videos.**—Files illustrate the results of CFD simulations using our *Pteridinium simplex* base model and 2 null models; provided as .gif files.

## Literature Cited

- Bardina, J. E., P. G. Huang, and T. J. Coakley. 1997. Turbulence modeling validation, testing, and development. NASA Technical Memorandum 110446:1–88.
- Bernard, F. R. 1974. Particle sorting and labial palp function in the Pacific oyster *Crassostrea gigas* (Thunberg, 1795). *Biology Bulletin* 146:1–10.
- Blazek, J. 2001. *Computational fluid dynamics: principles and applications*. Elsevier, Amsterdam.
- Bobrovskiy, I., J. M. Hope, E. Golubkova, and J. J. Brocks. 2020. Food sources for the Ediacara biota communities. *Nature Communications* 11:1261.
- Buss, L. W., and A. Seilacher. 1994. The Phylum Vendobionta: a sister group of the Eumetazoa? *Paleobiology* 20:1–4.
- Butman, C. A., M. Frechette, W. R. Geyer, and V. R. Starczak. 1994. Flume experiments on food supply to the blue mussel *Mytilus edulis* L. as a function of boundary-layer flow. *Limnology and Oceanography* 39:1755–1768.
- Butterfield, N. 2020. Constructional and functional anatomy of Ediacaran rangeomorphs. *Geological Magazine* 1–12. doi:10.1017/S0016756820000734.
- Clapham, M., G. M. Narbonne, and J. Gehling. 2003. Paleoeology of the oldest known animal communities: Ediacaran assemblages at Mistaken Point, Newfoundland. *Paleobiology* 29:527–544.
- Cracknell, K., D. C. Garcia-Bellido, J. G. Gehling, M. J. Ankor, S. A. F. Darroch, and I. A. Rahman. 2021. Pentaradial eukaryote suggests expansion of suspension feeding in White Sea-aged Ediacaran communities. *Scientific Reports* 11:4121.
- Crimes, T. P., and M. A. Fedonkin. 1996. Biotic changes in platform communities across the Precambrian–Phanerozoic boundary. *Rivista Italiana di Paleontologia e Stratigrafia* 102:317–332.
- Cunningham, J. A., I. A. Rahman, S. Lautenschlager, E. J. Rayfield, and P. C. J. Donoghue. 2014. A virtual world of paleontology. *Trends in Ecology and Evolution* 29:347–357.
- Darroch, S. A. F., E. A. Sperling, T. Boag, R. A. Racicot, S. J. Mason, A. S. Morgan, S. Tweedt, P. Myrow, D. H. Erwin, and M. Laflamme. 2015. Biotic replacement and mass extinction of the Ediacara biota. *Proceedings of the Royal Society of London B* 282:20151003.
- Darroch, S. A. F., T. Boag, R. A. Racicot, S. Tweedt, S. J. Mason, D. H. Erwin, and M. Laflamme. 2016. A mixed Ediacaran–metazoan assemblage from the Zaris Sub-basin, Namibia. *Palaeogeography, Palaeoclimatology, Palaeoecology* 459:198–208.
- Darroch, S. A. F., I. A. Rahman, B. M. Gibson, R. A. Racicot, and M. Laflamme. 2017. Inference of facultative mobility in the enigmatic Ediacaran organism *Parvancorina*. *Biology Letters* 13:20170033.
- Darroch, S. A. F., M. Laflamme, and P. J. Wagner. 2018a. High ecological complexity in benthic Ediacaran ecosystems. *Nature Ecology and Evolution* 2:1541–1547.
- Darroch, S. A. F., E. F. Smith, M. Laflamme, and D. H. Erwin. 2018b. Ediacaran extinction and Cambrian Explosion. *Trends in Ecology and Evolution* 33:653–663.
- Darroch, S. A. F., A. T. Cribb, L. A. Buatois, G. J. B. Germs, C. G. Kenchington, E. F. Smith, H. Mocke, G. R. O’Neil, J. D. Schiffbauer, K. M. Maloney, R. A. Racicot, K. A. Turk, B. M. Gibson, J. Almond, B. Koester, T. M. Boag, S. M. Tweedt,

- and M. Laflamme. 2020. The trace fossil record of the Nama Group, Namibia: exploring the terminal Ediacaran roots of the Cambrian explosion: *Earth-Science Reviews* 212:103435
- Decechi, T. A., G. M. Narbonne, C. Greentree, and M. Laflamme. 2017. Relating Ediacaran fronds. *Paleobiology* 43:171–180.
- Droser, M. L., and J. G. Gehling. 2015. The advent of animals: the view from the Ediacaran. *Proceedings of the National Academy of Sciences USA* 112:4865–4870.
- Droser M. L., J. G. Gehling, and S. R. Jensen. 2006. Assemblage palaeoecology of the Ediacara biota: The unabridged edition? *Palaeogeography, Palaeoclimatology, Palaeoecology* 232:131–147.
- Dunn, F. S., A. G. Liu, and P. C. J. Donoghue. 2018. Ediacaran developmental biology. *Biological Reviews* 93:914–932.
- Dunn, F. S., A. G. Liu, D. V. Grazhdankin, P. Vixseboxse, J. Flannery-Sutherland, E. Greem, S. Harris, P. R. Wilby, and P. C. J. Donoghue. 2021. The developmental biology of *Charnia* and the eumetazoan affinity of the Ediacaran rangeomorphs. *Science Advances* 7:eabe0291.
- Elliott, D. A., P. Vickers-Rich, P. W. Trusler, and M. Hall. 2011. New evidence on the taphonomic context of the Ediacaran *Pteridium*. *Acta Palaeontologica Polonica* 56:641–650.
- Elliott, D. A., P. W. Trusler, G. M. Narbonne, P. Vickers-Rich, N. Morton, M. Hall, K. H. Hoffmann, and G. I. C. Schneider. 2016. *Ernietta* from the late Ediacaran Nama Group, Namibia. *Journal of Paleontology* 90:1017–1026.
- Erwin, D. H., M. Laflamme, S. M. Tweedt, E. A. Sperling, D. Pisani, and K. J. Peterson. 2011. The Cambrian conundrum: early divergence and later ecological success in the early history of animals. *Science* 334:1091–1097
- Fedonkin, M. A. 1981. *Byelomorskaya biota Vend (White Sea biota of Vendian)*. Trudy Geologicheskii Institut Akademia Nauk S.S.S.R., Moscow.
- Fedonkin, M. A. 1990. Non-skeletal fauna of the Vendian: promorphological analysis. Pp. 7–120 in B. S. Sokolov and A. B. Iwanowski, eds. *The Vendian system. Vol. 1, Paleontology*. Springer-Verlag, Berlin.
- Fedonkin, M. A., and A. Y. Ivantsov. 2007. *Ventogyrus*, a possible siphonophore-like trilobozoan coelenterate from the Vendian Sequence (late Neoproterozoic), northern Russia. In P. Vickers-Rich and P. Komarower, eds. *The rise and fall of the Ediacaran biota*. Geological Society of London Special Publication 286:187–194.
- Gehling, J. G. 1991. The case for Ediacaran fossil roots to the metazoan tree. *Geological Society of India Memoir* 20:181–224.
- Gehling, J. G., and B. Runnegar. 2021. *Phyllozoon* and *Aulozoon*: key components of a novel Ediacaran death assemblage in Bathub Gorge, Heysen Range, South Australia. doi: 10.1017/S0016756821000509.
- Gibson, B. M., I. A. Rahman, K. Maloney, R. A. Racicot, H. Mocke, M. Laflamme, and S. A. F. Darroch. 2019. Gregarious suspension feeding in a modular Ediacaran organism. *Science Advances* 5: eaaw0260.
- Gibson, B. M., S. A. F. Darroch, K. M. Maloney, and M. Laflamme. 2021a. The importance of size and location within gregarious populations of *Ernietta plateauensis*. *Frontiers in Earth Science* 9. doi: 10.3389/feart.2021.749150.
- Gibson, B. M., D. J. Furbish, I. A. Rahman, M. W. Schmeekle, M. Laflamme, and S. A. F. Darroch. 2021b. Ancient life and moving fluids. *Biological Reviews* 96:129–152.
- Glaessner, M. F. 1959a. The oldest fossil faunas in South Australia. *Geologische Rundschau* 47:522–531.
- Glaessner, M. F. 1959b. Precambrian Coelenterata from Australia, Africa, and England. *Nature* 183:1472–1473.
- Glaessner, M. F. 1979. Biogeography and biostratigraphy: Precambrian. Pp. 79–118 in R. C. Moore (founder), R. A. Robinson, and C. Teichert, eds. *Introduction, fossilization (taphonomy), biogeography and biostratigraphy. Part A of R. C. Moore and C. Teichert, eds. Treatise on invertebrate paleontology Geological Society of America Boulder, Colo., and University of Kansas Press, Lawrence.*
- Glaessner, M. F., and M. Wade. 1966. The late Precambrian fossils from Ediacara, South Australia. *Palaeontology* 9:599–628.
- Grazhdankin, D. 2014. Patterns of evolution of the Ediacaran soft-bodied biota. *Journal of Paleontology* 88:269–283.
- Grazhdankin, D., and A. Seilacher. 2002. Underground Vendobionta from Namibia. *Palaeontology* 45:57–78.
- Grotzinger, J. P., and R. Miller. 2008. The Nama Group. In R. Miller, ed. *The geology of Namibia, Vol. 2. Geological Society of Namibia Special Publication* 13-229–13-272.
- Grotzinger, J. P., S. A. Bowring, B. Z. Saylor, and A. J. Kaufman. 1995. Biostratigraphic and geochronologic constraints on early animal evolution. *Science* 270:598–604.
- Gürich, G. 1929. Die ältesten Fossilien Südafrikas. In: *Zeitschrift praktische Geologie mit besonderer Berücksichtigung der Lagerstättenkunde* 37(6):85.
- Gürich, G. 1930a. Die bislang ältesten Spuren von Organismen in Südafrika. Pp. 670–680 in C.R. 15. *International Geological Congress, South Africa, 1929.*
- Gürich, G. 1930b. Über den Kuibisquarzit in Südwestafrika. *Zeitschrift Deutsch Geologie Gesellschaft* 82:637.
- Gürich, G. 1933. Die Kuibis-Fossilien der Nama-Formation von Südwestafrika. Nachträge und Zusätze. *Palaeontologische Zeitschrift* 15:137–154.
- Hall, M., A. J. Kaufman, P. Vickers-Rich, A. Ivantsov, P. W. Trusler, U. Linnemann, M. Hofmann, D. Elliott, C. Cui, M. Fedonkin, K.-H. Hoffmann, S. A. Wilson, G. Schneider, and J. Smith. 2013. Stratigraphy, palaeontology and geochemistry of the late Neoproterozoic Aar Member, southwest Namibia: reflecting environmental controls on Ediacara fossil preservation during the terminal Proterozoic in African Gondwana. *Precambrian Research* 238:214–232.
- Hoyal-Cuthill, J. F., and J. Han. 2018. Cambrian petalonamid *Stromatoveris* phylogenetically links Ediacaran biota to later animals. *Palaeontology* 61:813–823.
- Ivantsov, A. Y., and M. A. Fedonkin. 2002. Conulariidlike fossil from the Vendian of Russia: a metazoan clade across the Proterozoic/Palaeozoic boundary. *Palaeontology* 45:1219–1229.
- Ivantsov, A. Y., G. M. Narbonne, P. W. Trusler, C. Greentree, and P. Vickers-Rich. 2016. Elucidating *Erniettia*: new insights from exceptionally preserved specimens in the Ediacaran of Namibia. *Lethaia* 49:540–554.
- Jenkins, R. J. F. 1985. The enigmatic Ediacaran (late Precambrian genus) *Rangaea* and related forms. *Paleobiology* 11:336–355.
- Jenkins, R. J. F., and J. G. Gehling. 1978. A review of the frond-like fossils of the Ediacara assemblage. *Records of the South Australian Museum* 17:347–359.
- Jensen, S., and B. N. Runnegar. 2005. A complex trace fossil from the Spitskopf Member (terminal Ediacaran–Lower Cambrian) of Southern Namibia. *Geological Magazine* 142:561–569.
- Keller, B. M., V. V. Menner, V. A. Stepanov, and N. M. Chumakov. 1974. New finds of fossils in the Precambrian Valday Series along the Syuzma River. *Izvestia Akademii Nauk SSSR, Serya Geologicheskaya* 12:130–134.
- Klein, H. 2002. Current Statistics German Bight. BSH/DHI Current Measurements 1957–2001. Bundesamt für Seeschifffahrt und Hydrographie, Interner Bericht.
- Klein, H., and S. Dick. 1999. Currents at the light-vessel “Deutsche Bucht”: a comparison between ADCP measurements and the BSH forecast model. *Deutsche Hydrografische Zeitschrift* 51:465–475.
- Klein, H., and E. Mittelstaedt. 1991. Local currents at a shoreface-connected ridge in the German Bight. *Deutsche Hydrografische Zeitschrift* 44:133–142.

- Klein, H., P. König, and A. Frohse. 1999. Currents and near-bottom suspended matter dynamics in the central North Sea during stormy weather—results of the PIPE'98 field experiment. *Deutsche Hydrografische Zeitschrift* 51:47–66.
- LaBarbera, M. 1984. Feeding currents and particle capture mechanisms in suspension feeding animals. *American Zoologist* 24:71–84.
- Laflamme, M., and G. M. Narbonne. 2008a. Competition in a Precambrian world: palaeoecology of Ediacaran fronds. *Geology Today* 24:182–187.
- Laflamme, M., and G. M. Narbonne. 2008b. Ediacaran fronds. *Palaeogeography, Palaeoclimatology, Palaeoecology* 258:162–179.
- Laflamme, M., S. Xiao, and M. Kowalewski. 2009. Osmotrophy in modular Ediacara organisms. *Proceedings of the National Academy of Sciences USA* 106:14438–14443.
- Laflamme, M., S. A. F. Darroch, S. Tweedt, K. J. Peterson, and D. H. Erwin. 2013. The end of the Ediacara biota: extinction, biotic replacement, or Cheshire Cat? *Gondwana Research* 23:558–573.
- Lerosey-Aubril, R., and S. Pates. 2018. New suspension-feeding radiodont suggests evolution of microplanktivory in Cambrian macronekton. *Nature Communications* 9:3774.
- Linnemann, U., M. Ovtcharova, U. Schaltegger, A. Gartner, M. Hautmann, G. Geyer, P. Vickers-Rich, T. Rich, B. Plessen, M. Hofmann, J. Zieger, R. Krause, L. Kriesfeld, and J. Smith. 2019. New high-resolution age data from the Ediacaran–Cambrian boundary indicate rapid, ecologically driven onset of the Cambrian explosion. *Terra Nova* 31:49–58.
- Liu, A. G., C. G. Kenchington, and E. G. Mitchell. 2015. Remarkable insights into the paleoecology of the Avalonian Ediacaran macrobiota. *Gondwana Research* 27:1355–1380.
- Maloney, K. M., T. H. Boag, A. J. Faccioli, B. M. Gibson, A. Cribb, B. E. Koester, C. G. Kenchington, R. A. Racicot, S. A. F. Darroch, and M. Laflamme. 2020. Paleoenvironmental analysis of *Ernieittia*-bearing Ediacaran deposits in southern Namibia. *Palaeogeography, Palaeoclimatology, Palaeoecology* 556:109884.
- Meert, J. G., and B. S. Lieberman. 2008. The Neoproterozoic assembly of Gondwana and its relationship to the Ediacaran–Cambrian radiation. *Gondwana Research* 14:5–21.
- Meyer, M., D. Elliott, J. D. Schiffbauer, M. Hall, K.-H. Hoffman, G. Schneider, P. Vickers-Rich, and S. Xiao. 2014a. Taphonomy of the Ediacaran fossil *Pteridinium simplex* preserved three-dimensionally in mass flow deposits, Nama Group, Namibia. *Journal of Paleontology* 88:240–252.
- Meyer, M., D. Elliott, A. D. Wood, N. F. Polys, M. Colbert, J. A. Maisano, P. Vickers-Rich, M. Hall, K.-H. Hoffman, G. Schneider, and S. Xiao. 2014b. Three-dimensional microCT analysis of the Ediacara fossil *Pteridinium simplex* sheds new light on its ecology and phylogenetic affinity. *Precambrian Research* 249:79–87.
- Mitchell, E. G., and C. G. Kenchington. 2018. The utility of height for the Ediacaran organisms of Mistaken Point. *Nature Ecology and Evolution* 2:1218–1222.
- Mitchell, E. G., C. G. Kenchington, A. G. Liu, J. J. Matthews, and N. J. Butterfield. 2015. Reconstructing the reproductive mode of an Ediacaran macro-organism. *Nature* 524:343–346.
- Muscente, A. D., N. Bykova, T. H. Boah, L. A. Buatois, G. M. Mangano, A. Eleish, A. Prabh, F. Pan, M. B. Meyer, J. D. Schiffbauer, P. Fox, R. M. Hazen, and A. H. Knoll. 2019. Ediacaran biozones identified with network analysis provide evidence for pulsed extinctions of early complex life. *Nature Communications* 10:911.
- Narbonne, G. M., B. Z. Saylor, and J. P. Grotzinger. 1997. The youngest Ediacaran fossils from southern Africa. *Journal of Paleontology* 71:953–967.
- Pacheco, M. L. A. F., D. Galante, F. Rodrigues, J. D. M. Leme, P. Bidola, J. W. Hagadorn, M. Stockmar, J. Herzen, I. D. Rudnitzki, F. Pfeiffer, and A. C. Marques. 2015. Insights into the skeletonization, lifestyle, and affinity of the unusual Ediacaran fossil *Corumbella*. *PLoS ONE* 10:e0114219.
- Penny, A. M., R. A. Wood, A. Curtis, F. T. Bowyer, R. Tostevin, and K.-H. Hoffman. 2014. Ediacaran metazoan reefs from the Nama Group, Namibia. *Science* 344:1504–1506.
- Pflug, H. D. 1970a. Zur Fauna der Nama-Schichten in Südwest Afrika I. Pteridinia, Bau und Systematische Zugehörigkeit. *Palaeontographica* A134:226–262.
- Pflug, H. D. 1970b. Zur Fauna der Nama-Schichten in Südwest-Afrika. II. Rangeidae, Bau und Systematische Zugehörigkeit. *Palaeontographica* A135:198–231.
- Pflug, H. D. 1972a. Systematik der jung-präkambrischen Petalonamae Pflug 1970. *Palaeontologische Zeitschrift* 46:56–67.
- Pflug, H. D. 1972b. Zur Fauna der Nama-Schichten in Südwest-Afrika. III. Ernieittomorpha, Bau und Systematik. *Palaeontographica* A139:134–170.
- Pflug, H. D. 1973. Zur fauna der Nama-Schichten in Südwest-Afrika. IV. Mikroskopische anatomie der petalo-organismen. *Palaeontographica* B144:166–202.
- Rahman, I. A. 2017. Computational fluid dynamics as a tool for testing functional and ecological hypotheses in fossil taxa. *Palaeontology* 60:451–459.
- Rahman, I. A., S. A. F. Darroch, R. A. Racicot, and M. Laflamme. 2015. Suspension feeding in the enigmatic Ediacaran organism *Tribrachidium* demonstrates complexity of Neoproterozoic ecosystems. *Science Advances* 1:e1500800.
- Richter, R. 1955. Die ältesten Fossilien Süd-Afrikas. *Senckenbergiana Lethaia* 36:243–89.
- Runnegar, B. 2021. Following the logic behind biological interpretations of the Ediacaran biotas. *Geological Magazine*. doi: 10.1017/S0016756821000443.
- Saylor, B. Z., J. P. Grotzinger, and G. J. B. Germs. 1995. Sequence stratigraphy and sedimentology of the Neoproterozoic Kuibis and Schwarzrand Subgroups (Nama Group), southwestern Namibia. *Precambrian Research* 73:153–171.
- Schiffbauer, J. D., J. W. Huntley, G. R. O'Neil, S. A. F. Darroch, M. Laflamme, and Y. Cai. 2016. The latest Ediacaran wormworld fauna: setting the ecological stage for the Cambrian explosion. *GSA Today* 26:4–11.
- Schönberg, C. 2016. Happy relationships between marine sponges and sediments—a review and some observations from Australia. *Journal of the Marine Biological Association of the United Kingdom* 96:493–514.
- Seilacher, A. 1992. Vendobionta and Psammocorallia: lost constructions of Precambrian evolution. *Geological Society of London Special Publication* 149:607–613.
- Seilacher, A., and A. D. Gishlick. 2014. Vendobionts: lost life forms of Ediacaran times. Pp. 133–148 in A. Seilacher and A. D. Gishlick, eds. *Morphodynamics*. CRC Press, Taylor & Francis Group, Boca Raton, Fla.
- Shore, A. J., R. A. Wood, I. B. Butler, A. Y. Zhuravlev, S. McMahon, S. Curtis, S., and F. T. Bowyer. 2021. Ediacaran metazoan reveals lophotrochozoan affinity and deepens root of Cambrian explosion. *Science Advances* 7:eabf2933.
- Singer, A., R. Plotnick, and M. Laflamme. 2012. Experimental fluid mechanics of an Ediacaran frond. *Palaeontologia Electronica* 15:19A.
- Smits, A. J., and D. H. Wood. 1985. The response of turbulent boundary layers to sudden perturbations. *Annual Review of Fluid Mechanics* 17:321–358.
- Sperling, E.A., K. J. Peterson, and M. Laflamme. 2011. Rangeomorphs, *Thectardis* (Porifera?) and dissolved organic carbon in the Ediacaran ocean. *Geobiology* 9:24–33.

- Vickers-Rich, P., A.-Y. Ivantsov, P. W. Trusler, G. M. Narbonne, M. Hall, S. A. Wilson, C. Greentree, M. A. Fedonkin, D. Elliott, K.-H. Hoffmann, and G. I. C. Schneider. 2013. Reconstructing *Rangia*: new discoveries from the Ediacaran of Southern Namibia. *Journal of Palaeontology* 87:1–15.
- Vogel, S. 1994. *Life in moving fluids: the physical biology of flow*. Princeton University Press, Princeton, N.J.
- Wood, R., and A. Curtis. 2014. Extensive metazoan reefs from the Ediacaran Nama Group, Namibia: the rise of benthic suspension feeding. *Geobiology* 13:112–122.
- Wood, R. A., J. P. Grotzinger, and J. A. D. Dickson. 2002. Proterozoic modular biomineralized metazoan from the Nama Group, Namibia. *Science* 296:2383–2386.
- Wood, R. A., S. W. Poulton, A. R. Prave, K.-H. Hoffmann, M. O. Clarkson, R. Guilbaud, J. W. Lyne, R. Tostevin, F. Bowyer, A. M. Penny, A. Curtis, and S. A. Kasemann. 2015. Dynamic redox conditions control late Ediacaran metazoan ecosystems in the Nama Group, Namibia. *Precambrian Research* 261:252–271.
- Wood, R., A. G. Liu, F. Bowyer, P. R. Wilby, F. S. Dunn, C. G. Kenchington, J. F. Hoyal Cuthill, E. G. Mitchell, and A. Penny. 2019. Integrated records of environmental change and evolution challenge the Cambrian explosion. *Nature Ecology and Evolution* 3:528–538.
- Xiao, S., and M. Laflamme. 2009. On the eve of animal radiation: phylogeny, ecology and evolution of the Ediacara biota. *Trends in Ecology and Evolution* 24:31–40.